Mechanistic Studies of the Palladium(II)-Catalyzed Copolymerization of Ethylene with Carbon Monoxide

Francis C. Rix, Maurice Brookhart,* and Peter S. White

Contribution from the Department of Chemistry, The University of North Carolina at Chapel Hill, Chapel Hill, North Carolina 27599-3290

Received September 25, 1995[⊗]

Abstract: The microscopic steps responsible for the perfectly alternating copolymerization of ethylene and CO catalyzed by 1,10-phenanthroline (phen) based palladium complexes have been studied. Palladium carbonyl alkyl, carbonyl acyl, ethylene alkyl, and ethylene acyl complexes [(phen)Pd(R)(L)$^+$Ar′$_4$B$^-$ (Ar′ = 3,5-(CF$_3$)$_2$C$_6$H$_3$; R, L = CH_3, CO (**2**); CH_3, C_2H_4 (**3**); CH_2CH_3, C_2H_4 (**7**); $C(O)CH_3$, CO (**8**); $C(O)CH_3$, C_2H_4 (**13**); $CH_2CH_2C(O)CH_3$, C_2H_4 (**15**); $CH_2CH_2C(O)CH_3$, CO (**16**); $C(O)CH_2CH_2C(O)CH_3$, C_2H_4 (**17**); $C(O)CH_2CH_2C(O)CH_3$, CO (**18**)); and the β- and γ-keto chelate complexes (phen)Pd$CH_2CH_2C(O)CH_3^+$ (**14**) and (phen)Pd$C(O)CH_2CH_2C(O)CH_3^+$ (**19**)] have been prepared. An X-ray structure of the carbonyl acyl complex (phen)Pd($C(O)CH_3$)(CO)$^+$Ar′$_4$B$^-$·CH_2Cl_2 (**8**·CH_2Cl_2) has been obtained. The migratory insertion reactions of **2**, **3**, **7**, **13**, **16**, and **17** have been studied by low-temperature NMR techniques. The barriers for insertion increase in the following order: $\Delta G^{\ddagger}_{R\rightarrow CO} \approx 15$ kcal/mol (−66 °C) < $\Delta G^{\ddagger}_{Ac\rightarrow C_2H_4} \approx 17$ kcal/mol (*ca.* −45 °C) < $\Delta G^{\ddagger}_{R\rightarrow C_2H_4} \approx 19$ kcal/mol (−25 °C). The relative binding affinities of ethylene and CO to Pd methyl, acyl, and chelate complexes have been determined by combining stepwise measurements of the binding affinities of ligands with intermediate strength to (phen)Pd$(CH_3)(L)^+$ (CO > MeSPh > $CH_3CN \approx C_2H_4 > C_6H_5CN \gg OEt_2$) with relative equilibrium constants for ethylene/CO binding between acyl and alkyl complexes. The copolymerization mechanism has been determined from the kinetic and thermodynamic data. The catalyst resting state is a carbonyl acyl complex which is in equilibrium (K_5(25 °C) = (7.1 ± 3.5) × 10^{-4}) with a less stable ethylene acyl intermediate which undergoes β-acyl migratory insertion to generate a Pd alkyl species followed by rapid reaction with 2 equiv of CO to reform the resting state. This model is tested by comparing calculated and experimental turnover frequencies.

Introduction

The palladium-catalyzed perfectly alternating copolymerization of olefins with carbon monoxide is a currently active area of investigation.[1−3] Interest in these polymers, particularly the ethylene/CO copolymer (T_m = 257 °C),[2] stems from their unusual properties, the low cost of monomers, the presence of carbonyl functionality, and the potential for further functionalization along the backbone.[4,5] The mechanism of the copolymerization is of interest in its own right. The migratory insertion reactions responsible for chain growth, alkyl migration to CO, and acyl migration to olefins are members of a larger class of migratory insertion reactions that constitute key steps of transition metal catalyzed C−C bond-forming reactions in processes such as hydroformylation, hydroesterification, olefin oligomerization, and polymerization.[6−10] Of these reactions, the alkyl migration to CO is the most completely examined.[7] Direct observation of the migratory insertion reactions of olefin alkyl complexes is still rare;[11−21] a similar rearrangement of an ethylene acyl complex has only recently been directly monitored.[21] We have reported that the copolymerization of *p-tert*-butylstyrene with CO forms a high molecular weight copolymer with narrow molecular weight distributions ($\langle M_w\rangle/\langle M_n\rangle$ = 1.04 to 1.08).[22] This indicates that termination of polymerization does not compete with chain propagation. The absence of metal−carbon bond cleavage steps allows investigation of the roles that the migratory insertion reactions and the competition between CO and olefin binding to palladium play in C−C bond formation. This information is significant for understanding not only the copolymerization but also many other late transition metal-catalyzed olefin insertion and carbonylation reactions.

The copolymerization is commonly achieved in methanol solvent under high CO pressures using precatalysts formed *in*

[⊗] Abstract published in *Advance ACS Abstracts,* April 1, 1996.

(1) Sen, A. *Acc. Chem. Res.* **1993**, *26*, 303.
(2) Drent, E.; van Broekhaven, J. A. M.; Doyle, M. J. *J. Organomet. Chem.* **1991**, *417*, 235.
(3) Sen, A. *Adv. Polym. Sci.* **1986**, *73/74*, 125.
(4) Sen, A.; Jiang, Z.; Chen, J.-T. *Macromolecules* **1989**, *22*, 2012.
(5) Siddharth, S.; Jiang, Z.; Sen, A. *Polym. Prepr.* **1993**, *34*, 378.
(6) Collman, J. P.; Hegedus, L. S.; Norton, J. R.; Finke, R. G. *Principles and Applications of Organotransition Metal Chemistry*; University Science Books: Mill Valley, CA, 1987.
(7) Colquhoun, H. M.; Thompson, D. J.; Twigg, M. V. *Carbonylation, Direct Synthesis of Carbonyl Compounds*; Plenum Press: New York, 1991.
(8) Parshall, G. W.; Ittel, S. D. *Homogeneous Catalysis*, 2nd ed.; Wiley: NY, 1992.
(9) Thorn, D. L.; Hoffmann, R. *J. Am. Chem. Soc.* **1978**, *100*, 2079.
(10) Samsel, E. G.; Norton, J. R. *J. Am. Chem. Soc.* **1984**, *106*, 5505.
(11) Cramer, R. *J. Am. Chem. Soc.* **1965**, *87*, 4717.
(12) Clark, H. C.; Jablonski, C. R.; Von Werner, K. *J. Organomet. Chem.* **1974**, *82*, C51.
(13) Pardy, R. A. *J. Organomet. Chem.* **1981**, *216*, C29.
(14) Flood, T. C.; Statler, J. A. *Organometallics* **1984**, *3*, 1795.
(15) Flood, T. C.; Bitler, S. P. *J. Am. Chem. Soc.* **1984**, *106*, 6076.
(16) Wang, L.; Flood, T. C. *J. Am. Chem. Soc.* **1992**, *114*, 3169.
(17) Ermer, S. P.; Struck, G. E.; Bitler, S. P.; Richards, R.; Bau, R.; Flood, T. C. *Organometallics* **1993**, *12*, 2634.
(18) Brookhart, M.; Lincoln, D. M. *J. Am. Chem. Soc.* **1988**, *110*, 8719.
(19) Brookhart, M.; Volpe, A. F.; Lincoln, D. M.; Hovarth, I. T.; Millar, J. M. *J. Am. Chem. Soc.* **1990**, *112*, 5634.
(20) Brookhart, M.; Hauptman, E. *J. Am. Chem. Soc.* **1992**, *114*, 4437. See also refs 42 and 43.
(21) Preliminary communication of this work: Rix, F. C.; Brookhart, M. *J. Am. Chem. Soc.* **1995**, *117*, 1137.
(22) Brookhart, M.; Rix, F. C.; DeSimone, J. M.; Barborak, J. C. *J. Am. Chem. Soc.* **1992**, *114*, 5894.

S0002-7863(95)03276-8 CCC: $12.00

situ from addition of a bidentate ligand to a weakly coordinated dicationic palladium complex such as $[Pd(NCMe)_4]^{2+}(BF_4^-)_2$.[2,23] Representative ligands include 1,3-bis(diphenylphosphino)-propane (DPPP) and 1,10-phenanthroline (phen). The active catalyst is monocationic; the dicationic precursors transform into monocationic palladium hydride or palladium carbomethoxy species prior to initiation of the polymerization. The most important chain termination steps involve formation of alkyl and ester polymer end groups from protonolysis of the metal−alkyl bond or methanolysis of the palladium−acyl bond.[1,2]

The copolymer forms by alternating migratory insertion reactions of carbonyl alkyl and olefin acyl complexes. Sen has proven the viability of these intermediates by initiation of the

$$L_nPd(CHRCH_2C(O)\text{-pol.})(CO)^+ \rightarrow L_nPd(C(O)CHRCH_2C(O)\text{-pol.})^+$$

$$L_nPd(C(O)CHRCH_2C(O)\text{-pol.})(CHR{=}CH_2)^+ \rightarrow L_nPd(CHRCH_2C(O)CHRCH_2C(O)\text{-pol.})^+$$

copolymerization with monocationic palladium alkyl and acetyl complexes.[24] Rival migratory insertion reactions of olefin alkyl and carbonyl acyl complexes do not compete with propagation. Sen has further demonstrated that double carbonylation is thermodynamically very unfavorable and has proposed that the higher affinity of palladium for CO relative to ethylene inhibits multiple ethylene insertions.[24−26] An alternative mechanism involving palladium carbene intermediates has been proposed to account for the isolation of a spiroketal polymer from these methanol-based copolymerizations.[27] Since this proposal, there has been increasing evidence that the spiroketal isomer forms after the alternating copolymer is formed.[1,22,28]

The migratory insertion of carbonyl alkyl complexes has been widely studied. However, the direct observation of this reaction at a palladium center has only recently been observed. Tòth and Elsevier have reported that (*S*,*S*-BDPP)Pd$(CH_3)(^{13}CO)^+BF_4^-$ (*S*,*S*-BDPP = (2*S*,4*S*)-bis(diphenylphosphino)pentane) reacts with ^{13}CO to yield (*S*,*S*-BDPP)Pd$(^{13}C(O)CH_3)(^{13}CO)^+BF_4^-$ under ^{13}CO pressure.[29] The reaction, which was followed by low-temperature ^{13}C NMR spectroscopy, is reported to proceed at the same rate under either atmospheric or 10 bar of CO pressure, although the rate constant was not disclosed. The lack of dependence of the rate on P_{CO} suggests that the reaction does not proceed by way of a five-coordinate intermediate or a bimolecular insertion, but instead most likely occurs by rate determining methyl migration to CO followed by CO trapping of the unsaturated acetyl intermediate.

The β-acyl migration to olefins has been reported to form chelated complexes of the type $L_2Pd\overline{CRHCR'HC(O)}R^+$.[30−34] The isolation of oligomeric chelate complexes from the copolymerization of norbornene and CO and the observation of 6-membered chelates $L_2Pd\overline{C(O)CHRCHR'C(O)}CH_3^+$ from reaction of the 5-membered chelates with CO has been reported.[35,36] The related β-carboalkoxy migration to acetylenes and olefin has also been studied.[10] However, the direct observation of olefin acyl complexes and their migratory insertion reactions have remained elusive. Similarly, the details of the mechanism of the copolymerization, in spite of the seeming simplicity of the alternating migratory insertion reactions, have not yet been fully elucidated. Very little has been reported regarding the identity of the resting state(s), the role of the carbonyl chelate complexes, and the magnitudes of the binding affinities of the possible ligands (CO, olefins, chelates, MeOH, and counteranion) in the *in situ* generated polymerizations.

We have examined the microscopic steps responsible for copolymerization of ethylene and CO initiated by the (phen)-Pd$(CH_3)(NCCH_3)^+$ precatalyst. The study has been simplified by using the polar aprotic solvent methylene chloride in combination with the bulky noncoordinating $(3,5\text{-}(CF_3)_2C_6H_3)_4B^-$ (Ar'_4B^-) counteranion. These two features eliminate equilibria involving solvent or counteranion coordination to palladium and methanolysis or protonolysis of palladium−carbon bonds. The high solubility of palladium salts incorporating the Ar'_4B^- anion at very low temperatures (<−100 °C) in CD_2Cl_2 permits low-temperature NMR studies to be conducted. Furthermore, induction periods associated with the transformation of dicationic precatalysts to active monocationic species[37] are eliminated with the well-defined (phen)Pd$(CH_3)(NCCH_3)^+$ initiators.

We report here a series of *in situ* low-temperature NMR studies of (1) the kinetics of directly observed migratory insertion reactions of carbonyl alkyl, ethylene acyl, and ethylene alkyl complexes[21] and (2) the relative binding affinities of ethylene versus carbon monoxide. The kinetic and thermodynamic data have been combined to construct an accurate model for copolymer chain growth that successfully predicts turnover frequencies for the ethylene/CO copolymerization.

Results and Discussion

1. Preparation of (phen)Pd$(CH_3)(L)^+$ (L = CO (2), C_2H_4 (3), $S(CH_3)(C_6H_5)$ (4), CH_3CN (5), C_6H_5CN (6)). The cationic ether adduct (phen)Pd$(CH_3)(OEt_2)^+$ (**1**) is an excellent starting material for other (phen)Pd$(CH_3)(L)^+$ complexes. The preparation and full characterization, including X-ray crystallography, of **1** has been reported separately.[38] The coordinated ether ligand is quite labile. The addition of L to **1** at −78 °C or above rapidly forms complexes **2**−**6** (Scheme 1). All of these complexes are isolated as solids with the exception of **3** which must be prepared *in situ* in CD_2Cl_2 at low temperature due to its facile irreversible β-CH_3 migratory insertion reaction. The relative binding affinities of this series of ligands have been determined and will be described shortly.

(23) Sen, A.; Jiang, Z. *Macromolecules* **1993**, *26*, 911.
(24) Lai, T.-W.; Sen, A. *Organometallics* **1984**, *3*, 866.
(25) Chen, J.-T.; Sen, A. *J. Am. Chem. Soc.* **1984**, *106*, 1506.
(26) Sen, A.; Chen, J.-T.; Vetter, W. M.; Whittle, R. R. *J. Am. Chem. Soc.* **1987**, *109*, 148.
(27) Batistini, A.; Consiglio, G. *Organometallics* **1992**, *11*, 1766.
(28) (a) Wong, P. K.; van Doorn, J. A.; Drent, E.; Sudmeijer, O.; Stil, H. A. *Ind. Eng. Chem. Res.* **1993**, *32*, 986. (b) Jiang, Z.; Sen, A. *J. Am. Chem. Soc.* **1995**, *117*, 4455.
(29) (a) Tòth, I.; Elsevier, C. J. *J. Am. Chem. Soc.* **1993**, *115*, 10388. (b) van Leeuwen, P. W. N. M.; Roobeek, K. F. *Recl. Trav. Chim. Pays-Bas.* **1995**, *114*, 73 and references therein.
(30) Brumbaugh, J. S.; Whittle, R. R.; Parvez, M.; Sen, A. *Organometallics* **1990**, *9*, 1735.
(31) For examples of migratory insertion of Pd acyl complexes see: Ozawa, F.; Hayashi, T.; Koide, H.; Yamamoto, A. *J. Chem. Soc., Chem. Commun.* **1991**, 1469.
(32) Dekker, G. P. C. M.; Buijs, A.; Elsevier, C. J.; Vrieze, K.; van Leeuwen, P. W. N. M.; Smeets, W. J. J.; Spek, A. L.; Wang, Y. F.; Stam, C. *Organometallics* **1992**, *11*, 1937.
(33) Dekker, G. P. C. M.; Elsevier, C. J.; Vrieze, K.; van Leeuwen, P. W. N. M. *Organometallics* **1992**, *11*, 1598.
(34) Markies, B. A.; Rietveld, M. H. P.; Boersma, J.; Spek, A. L.; van Koten, G. *J. Organomet. Chem.* **1992**, *424*, C12.
(35) van Asselt, R.; Gielens, E. E. C. G.; Rülke, R. E.; Vrieze, K.; Elsevier, C. J. *J. Am. Chem. Soc.* **1994**, *116*, 997.
(36) Markies, B. A.; Kruis, D.; Rietvald, M. H. P.; Verkerk, K. A. N.; Boersma, J.; Kooijman, H.; Lakin, M. T.; Spek, A. L.; van Koten, G. *J. Am. Chem. Soc.* **1995**, *117*, 5263.
(37) Jiang, Z.; Dahlen, G. M.; Houseknecht, K.; Sen, A. *Macromolecules* **1992**, *25*, 2999.
(38) Rix, F. C.; Brookhart, M.; White, P. S. *J. Am. Chem. Soc.* **1996**, *118*, 2436.

Scheme 1. Synthesis of (phen)Pd(CH_3)(L)$^+$Ar′$_4$B−

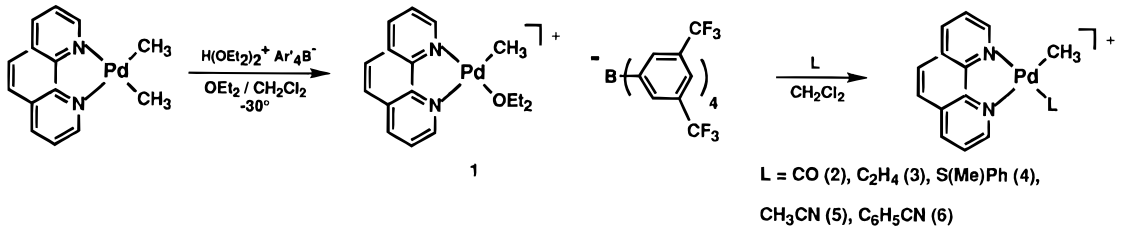

1

2. The β-R Migratory Insertion Chemistry of (phen)Pd(R)(C_2H_4)$^+$ (R = CH_3 (3), CH_2CH_3 (7)). The palladium adducts of carbon monoxide, **2**, and ethylene, **3**, model two important intermediates during the catalysis. The migratory insertion chemistry of the carbonyl methyl complex **2** is a potential model for one of the propagation steps in the copolymerization mechanism, while the ethylene methyl species **3** is of significance because consecutive olefin insertions do *not* occur during the copolymerization. Complex **3** is prepared *in situ* from the addition of ethylene to **1**. When <1 equiv of ethylene is added to **1**, the coordinated ethylene ligand displays a characteristic AA′BB′ pattern centered at δ 5.02 in the −110 °C (CD_2Cl_2/$CDCl_2F$) ^{1}H NMR spectrum and a single resonance at δ 86.4 (t, J_{CH} = 163 Hz) in the ^{13}C NMR spectrum. The olefinic multiplets collapse to a singlet as the temperature is raised. At the coalescence temperature, T_c, of −81 °C, k_{ex} = 162 ± 32 s^{-1} and $\Delta G^{\ddagger}$ = 9.2 ± 0.2 kcal/mol.[39] In order to observe the ethylene multiplets, the amount of ethylene added to **1** is critical. In the presence of a slight excess (0.5 equiv) of free ethylene, one singlet (δ 5.13) is observed for both the combined free and coordinated ethylene signals at −110 °C; the rest of the spectrum is unaffected. Thus, the presence of a small amount of free ethylene results in an extremely rapid associative ethylene exchange.

In the presence of excess ethylene, the clean conversion of **3** to propene and the ethyl ethylene complex (phen)Pd(C_2H_5)(C_2H_4)$^+$ (**7**) occurs at −25 °C. Complex **7** is the resting state of a catalytic system for ethylene dimerization (Scheme 2). Butene composition is relatively constant at high ethylene concentration: *trans*-2 (60−65%) > *cis*-2 (30−35%) > 1 (5−10%). The butene composition varied during the dimerization favoring *trans* at the expense of *cis*- and 1-butene as ethylene concentration decreased. After the ethylene was completely consumed, conversion of the butenes to higher order oligomers was observed.

The characterization of **7** is complicated since the observed NMR resonances represent an average of several exchanging olefin complexes, due to the presence of propene, excess ethylene, and butenes. This problem was overcome by condensing propane directly into a −78 °C CD_2Cl_2 solution of a working dimerization system and precipitating **7** as a thermally unstable off-white solid. After washing twice with propane and vacuum drying at −78 °C, ^{1}H and ^{13}C NMR analysis confirmed the presence of pure **7**. NMR data are similar to **3** (^{1}H: broad AA′BB′ centered at δ 5.0, −110 °C; ^{13}C: δ 87.0, J_{CH} = 161 Hz, −85 °C). The rate constant for exchange of the nonequivalent ethylene hydrogens of **7** at coalescence (T_c = −76 °C) is k = 306 ± 61 s^{-1}, $\Delta G^{\ddagger}$ = 9.2 ± 0.2 kcal/mol.

(39) There are several possible mechanisms for the exchange of the magnetically inequivalent ethylene hydrogens. Two possible intramolecular mechanisms are (i) ethylene rotation and (ii) π-bond slippage to an η^2-C−H ligand, rotation of the η^2-C−H bond (about the M−CH axis), and recoordination of the π bond. Intermolecular exchange may occur by reversible nucleophile-promoted ethylene displacement.

Scheme 2. The Direct Observation of the β-Alkyl Migratory Insertion Reactions of (phen)Pd(R)(C_2H_4)$^+$ (R = CH_3 (**3**), CH_2CH_3 (**7**))[a]

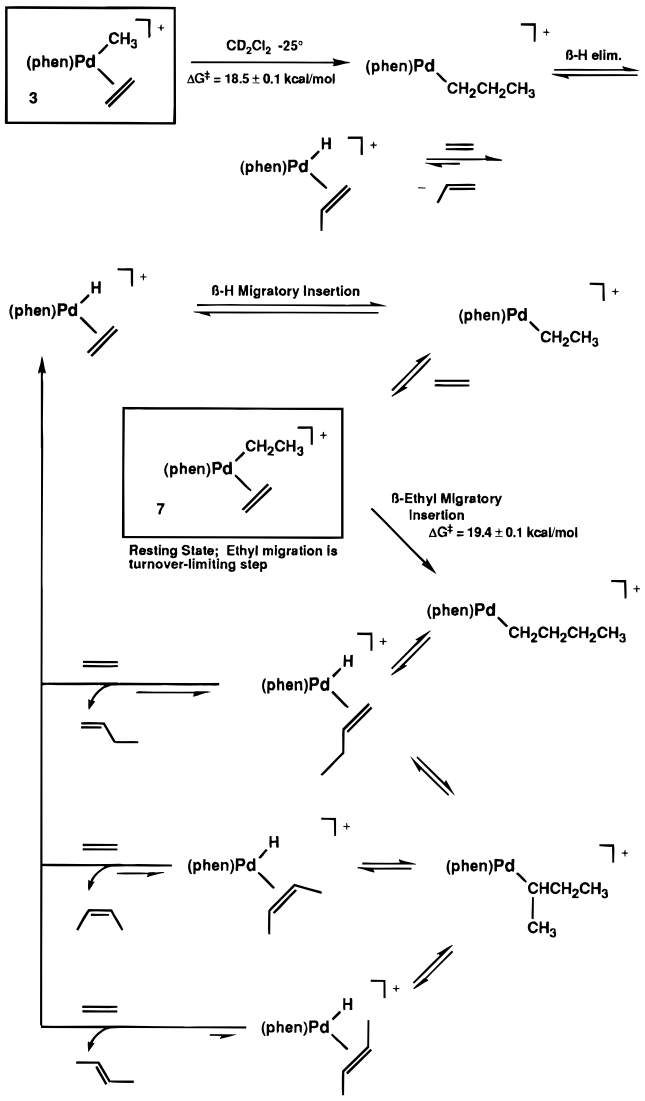

[a] The boxed compounds were directly observed; other species are proposed intermediates of the catalytic cycle for ethylene dimerization.

Complexes **3** and **7** allow direct comparison of the energetics of methyl and ethyl group migrations to ethylene. The rate constant for methyl migration was determined from the first-order decay of **3** by ^{1}H NMR spectroscopy. This rate constant is unchanged in the presence of 5, 12, or 20 equiv of ethylene, verifying that the insertion reaction is not bimolecular between **3** and ethylene. Since **7** is the resting state of an ethylene dimerization cycle, the rate constant for migratory insertion is equal to the turnover frequency of the catalytic cycle (Scheme 2). Linear plots of turnovers versus time were obtained even at high (80−100%) conversion of ethylene (Figure 1), indicating

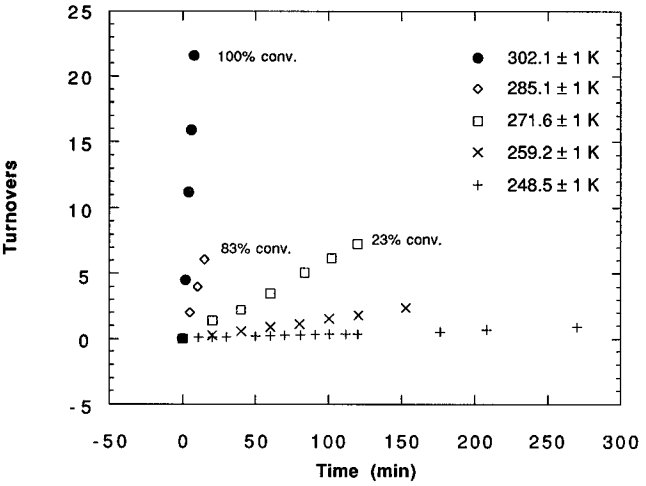

Figure 1. Linear plots of turnovers (moles of butenes/moles of catalyst) of the ethylene dimerization catalyzed by (phen)Pd(C_2H_5)(C_2H_4)$^+$, **7**, versus time in the temperature range 248.5 to 302.1 K.

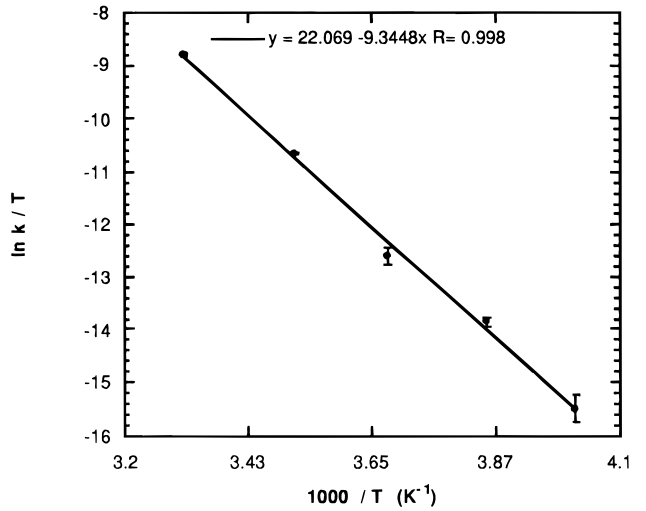

Figure 2. Eyring plot for the β-Et migratory insertion reaction of (phen)Pd$-$(CH_2CH_3)(C_2H_4)$^+$, from 248.5 K to 302.1 K, $\Delta H^{\ddagger} = 18.5 \pm 0.6$ kcal/mol, $\Delta S^{\ddagger} = -3.7 \pm 2.0$ eu.

that turnover rates are independent of ethylene concentration. An Eyring plot of this rate data, obtained over a 54 deg temperature range, gave $\Delta H^{\ddagger} = 18.5 \pm 0.6$ kcal/mol and $\Delta S^{\ddagger} = -3.7 \pm 2.0$ eu. The small $\Delta S^{\ddagger}$ is consistent with other reports of $\Delta S^{\ddagger}$ for β-H[40−42] and β-alkyl[16,17] migratory insertion reactions. The facts that (1) the resting state of the catalytic cycle is the ethylene ethyl complex **7**, (2) the turnover frequency is independent of [C_2H_4], and (3) $\Delta S^{\ddagger}$ is small clearly indicate that the rate-determining step in the catalytic cycle is ethyl migration to ethylene. Rate constants and $\Delta G^{\ddagger}$ values for these migratory insertion reactions at −25 °C are the following: $k_{Me\rightarrow C_2H_4} = (2.8 \pm 0.2) \times 10^{-4}$ s^{-1}, $\Delta G^{\ddagger}_{Me\rightarrow C_2H_4} = 18.5 \pm 0.1$ kcal/mol; $k_{Et\rightarrow C_2H_4} = (4.7 \pm 0.6) \times 10^{-5}$ s^{-1}, $\Delta G^{\ddagger}_{Et\rightarrow C_2H_4} = 19.4 \pm 0.1$ kcal/mol. The barrier for methyl migration is ca. 0.9 kcal/mol less than that for ethyl migration. A similar trend was observed in the related ethylene polymerization catalyst (ArN=C(R′)C(R′)=NAr)Pd(R)(C_2H_4)$^+$Ar′$_4$B$^-$ (R = Me, *n*-alkyl; R′ = H, alkyl).[43] This bias is reversed for Cp*-[($MeO)_3$P]Rh(C_2H_4)(R)$^+$ (R = CH_3, C_2H_5) complexes which display a 0.8 kcal/mol preference for ethyl, over methyl, migration.[42] In any case, the $\Delta\Delta G^{\ddagger}$ is modest and its origin is not easily determined. In order to connect these data with the

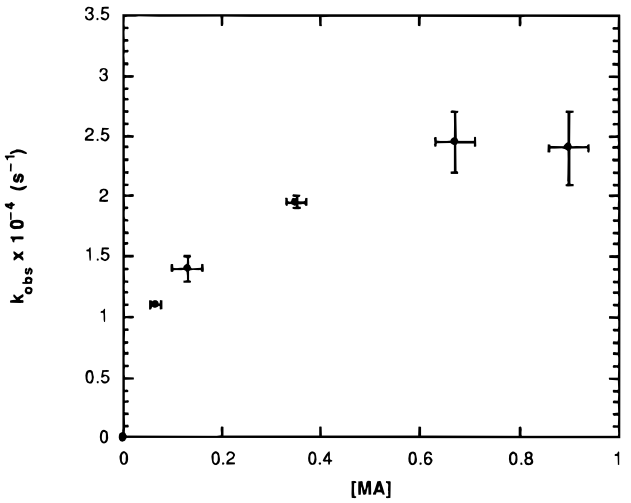

Figure 3. Saturation plot for the reaction (phen)Pd(CH_3)(CO)$^+$ (**2**) + MA → (phen)Pd$\overline{\text{CH(CO}_2\text{Me)CH}_2\text{C(O)}}Me^+$ (**9**).

larger goal of understanding the limited role of ethylene alkyl insertions in the copolymerization, the rate of the α-CH_3 migratory insertion reaction of the carbonyl methyl complex **2** and the relative binding affinities of CO and ethylene have been studied.

3. The α-CH_3 Migratory Insertion Chemistry of (phen)Pd(CH_3)(CO)$^+$ (2). (a) Preparation of 2. The carbonyl methyl complex, (phen)Pd(CH_3)(CO)$^+$ (**2**) is formed upon addition of CO to the ether complex **1** at −78 °C (Scheme 1). Precipitation by the addition of hexanes, followed by crystallization from a CH_2Cl_2/hexanes mixture yields pure **2**. The carbonyl resonance occurs at δ 176.3. The IR spectrum reveals a very high CO stretching frequency at 2130 cm^{-1}, indicating that complex **2** is very electrophilic with little dπ donation into the CO π* orbitals.[29,32,33,44]

There are several complications which arise in the preparation of **2**. First, if **1** is formed *in situ*, care must be taken not to "underprotonate" the (phen)Pd(CH_3)$_2$ precursor since it decomposes at 20 °C in the presence of CO or **2** in methylene chloride solutions. Additionally, **1** must be completely in solution at −78 °C to ensure its total conversion to **2**. Complex **1** decomposes in CH_2Cl_2 at room temperature and can interfere with the crystallization of **2**. Finally, even at −78 °C, **2** slowly reacts with CO to form the carbonyl acyl complex (phen)Pd(C(O)CH_3)(CO)$^+$ (**8**), requiring that **2** be precipitated from solution at −78 °C and afterwards crystallized from CH_2Cl_2/hexanes.

(b) Reaction of 2 with Methyl Acrylate. The migratory insertion chemistry of **2** was studied using a variety of trapping ligands. Complex **2** reacts with methyl acrylate (MA) at −66 °C to yield a very stable 5-membered palladacycle, (phen)Pd$\overline{\text{(CH(CO}_2\text{CH}_3\text{)CH}_2\text{C(O)CH}_3\text{)}}^+$ (**9**).[31] The metallacycle

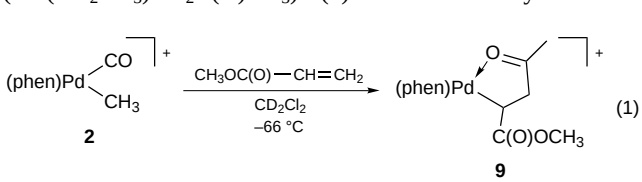

(1)

has been identified by the diagnostic ^{13}C resonance of the

(40) Doherty, N. M.; Bercaw, J. E. *J. Am. Chem. Soc.* **1985**, *107*, 2670.
(41) Burger, B. J.; Santarsiero, B. D.; Trimmer, M. S.; Bercaw, J. E. *J. Am. Chem. Soc.* **1988**, *110*, 3134.
(42) Brookhart, M.; Hauptman, E.; Lincoln, D. *J. Am. Chem. Soc.* **1992**, *114*, 10394.
(43) Johnson, L. K.; Killian, C. M.; Brookhart, M. *J. Am. Chem. Soc.* **1995**, *117*, 6414.
(44) For examples of *trans* acetone acyl Pd complexes see: Huang, L.; Ozawa, F.; Yamamoto, A. *Organometallics* **1990**, *9*, 2603.

chelated carbonyl at δ 241.0.[30] The regiochemistry of insertion was determined by analysis of the magnitudes of the carbon−carbon coupling constants for its ^{13}CO-labeled isotopomer, (phen)Pd(CH(CO$_2$CH$_3$)CH$_2$^{13}C(O)CH$_3$)$^+$, which displays $^1J_{CC}$ of *ca.* 41 Hz to the ^{13}CH$_3$ and ^{13}CH$_2$, and $^2J_{CC}$ of 2 Hz to ^{13}**C**HCO$_2$Me. Complex **9** does not react further with MA or CO at −66 °C. The clean conversion of **2** and MA to **9** was monitored by ^{1}H NMR spectroscopy. No intermediates were observed. The rate constants for this transformation were determined as a function of [MA]. A plot of k_{obs} vs [MA] for two averaged sets of data is shown in Figure 3. Displaying the classical saturation behavior often observed in carbonyl insertion chemistry, the k_{obs} increases and levels off to a limiting value ($k_{lim} = (2.4 \pm 0.3) \times 10^{-4}$ s^{-1}, $\Delta G^{\ddagger} = 15.4 \pm 0.1$ kcal/mol), with increasing [MA].[6] A mechanism for this reaction is proposed below. Under steady state conditions, α-CH$_3$ migratory

$$\underset{\mathbf{2}}{(\text{phen})\text{Pd}(\text{CH}_3)(\text{CO})^+} \underset{k_{-1}}{\overset{k_1}{\rightleftharpoons}} \underset{\mathbf{2\text{-}I}}{(\text{phen})\text{Pd}(\text{C(O)CH}_3)^+} \quad (2)$$

$$\underset{\mathbf{2\text{-}I}}{(\text{phen})\text{Pd}(\text{C(O)CH}_3)^+} + \text{MA} \xrightarrow{k_2} (\text{phen})\text{Pd}(\text{C(O)CH}_3)(\text{MA})^+ \quad (3)$$

$$(\text{phen})\text{Pd}(\text{C(O)CH}_3)(\text{MA})^+ \xrightarrow[>k_1]{\text{very fast}} \underset{\mathbf{9}}{(\text{phen})\text{PdCH}(\text{CO}_2\text{Me})\text{CH}_2\text{C(O)Me}^+} \quad (4)$$

insertion occurs to give the unsaturated acyl **2-I**. MA traps the vacant coordination site followed by extremely fast β-acetyl migratory insertion, such that MA trapping is irreversible, to give the metallacycle **9**. The rate expression for this reaction is

$$k_{obs} = k_1 k_2[\text{MA}]/(k_{-1} + k_2[\text{MA}])$$

In the limit where k_2[MA] $\gg k_{-1}$ the expression simplifies to

$$k_{obs} = k_1$$

Thus, k_{lim} equals k_1 and represents the rate constant for α-CH$_3$ migratory insertion of (phen)Pd(CH$_3$)(CO)$^+$.

(c) Reaction of 2 with CO. Complex **2** reacts with CO to form the carbonyl acetyl complex (phen)Pd(C(O)CH$_3$)(CO)$^+$ (**8**).[44] Complex **8**·CH$_2$Cl$_2$ was isolated by crystallization from CH$_2$Cl$_2$/hexane under a CO atmosphere. Once formed, the

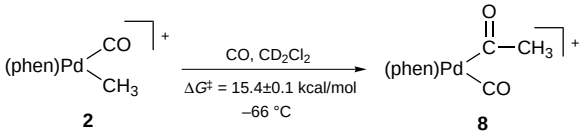

2 **8** (5)

crystals, **8**·CH$_2$Cl$_2$, are stable toward decarbonylation. Complex **8** displays two ^{13}C carbonyl resonances; the terminal CO is shifted *ca.* 2 ppm upfield from **2** to δ 174.1, and the acyl resonance occurs at δ 214.3 (20 °C). The IR spectrum displays carbonyl bands at 2128 cm^{-1} for the terminal CO and 1748 cm^{-1} for the acetyl carbonyl. The similarity of the ν_{CO}(terminal) to that of **2** (ν_{CO} = 2130 cm^{-1}) indicates that there is little difference in the back-bonding abilities of the two complexes upon substitution of methyl for acetyl. Crystals of **8**·CH$_2$Cl$_2$ suitable for X-ray diffraction have been obtained; an ORTEP drawing and key structural features are given in Figure 4 and Table 1. An interesting feature of the structure is the "upright" orientation of the acetyl group, perpendicular to the square plane.

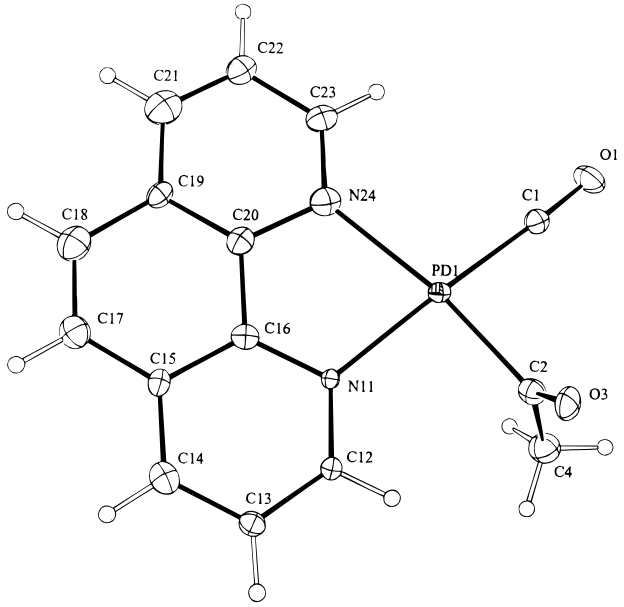

Figure 4. ORTEP structure of (phen)Pd(C(O)CH$_3$)(CO)$^+$Ar′$_4$B$^-$·CH$_2$Cl$_2$ (**8**·CH$_2$Cl$_2$). The Ar′$_4$B$^-$ counterion and CH$_2$Cl$_2$ are not shown for the sake of clarity. All atoms are drawn at 50% probability ellipsoids except for hydrogens which have been assigned arbitrary thermal parameters.

Table 1. Selected Bond Lengths (Å) and Angles (deg) for **8**·CH$_2$Cl$_2$

Pd1−C1	1.922 (11)	Pd1−N24	2.146 (10)
Pd1−C2	2.001 (12)	C1−O1	1.112 (14)
Pd1−O3	2.784 (08)	C2−O3	1.185 (14)
Pd1−N11	2.098 (08)	C2−C4	1.496 (17)
C1−Pd1−C2	87.2 (05)	C2−Pd1−N24	170.2 (04)
C1−Pd1−N11	175.7 (04)	N11−Pd1−N24	79.5 (03)
C1−Pd1−N24	102.4 (04)	Pd1−C1−O1	177.3 (10)
C2−Pd1−N11	90.9 (04)	Pd1−C2−O3	119.6 (09)
N11−Pd1−C2−C4	88.1 (07)		

This orientation has also been observed for olefin and carbene ligands in square-planar platinum olefin and carbene complexes[45] and also for the ether ligand in **1**.[38] Steric forces have been proposed to control these ligand orientations and presumably dictate the geometry of the acyl ligand here as well.

The reaction of **2** with CO was monitored by ^{1}H NMR spectroscopy. A 0.011 M solution of **2** was saturated with CO at −78 °C. The formation of **8** at −66 °C proceeds at the same rate as the formation of the metallacycle **9** in the saturation limit, but only to 55% completion. The calculated [CO] in a saturated CD$_2$Cl$_2$ solution at −66 °C is 6.3×10^{-3} M, about half the concentration of **2** used. Plots of the mole fraction of **8**, X(**8**), and ln(1 − X(**8**)) versus time illustrate this titration (Figure 5). This interesting development allows the [CO] dependence of the migratory insertion to be evaluated in a qualitative way. The natural log plot remains fairly linear while the CO in solution is consumed and gives a rate constant $k = 2.6 \times 10^{-4}$ s^{-1} which is equal to k_{lim} from the MA saturation kinetics study. Using a less concentrated solution of **2** allowed the reaction to be followed for 2 half-lives giving $k = 2.2 \times 10^{-4}$ s^{-1} and an average rate constant $k = (2.4 \pm 0.2) \times 10^{-4}$ s^{-1}, $\Delta G^{\ddagger} = 15.4 \pm 0.1$ kcal/mol. The fact that MA and CO, which must have widely different binding affinities, react with **2** at the same limiting rate justifies the previous assumption that trapping of **2-I** by MA is made irreversible by extremely rapid acetyl migration to MA.

(45) Albright, T. A.; Hoffmann, R.; Thibeault, J. C.; Thorn, D. L. *J. Am. Chem. Soc.* **1979**, *101*, 3801 and references therein.

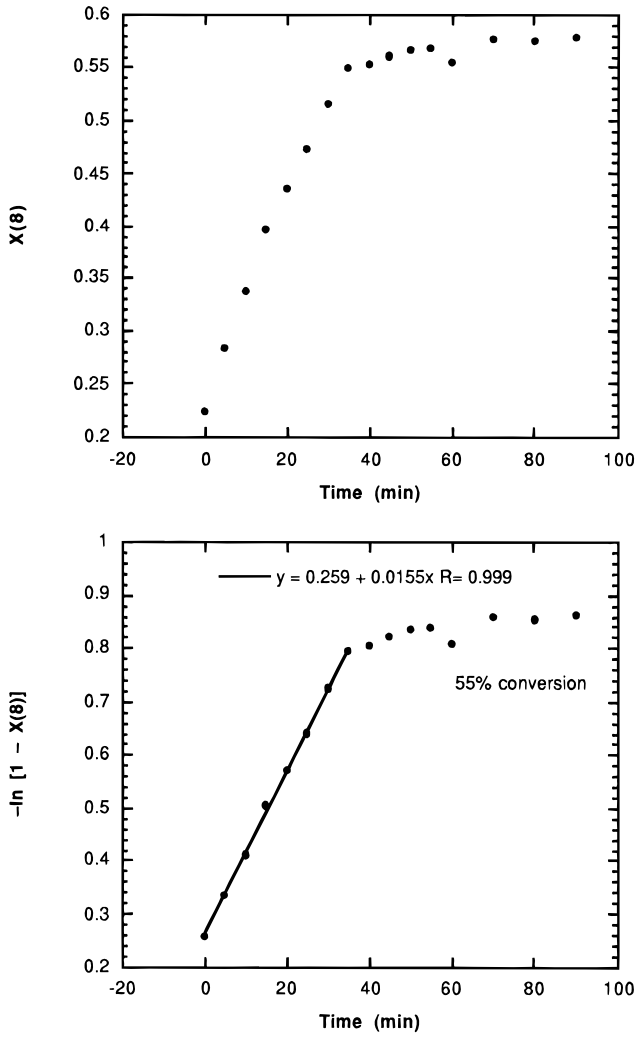

Figure 5. Plots of the mole fraction of **8**, X(**8**), and $-\ln[1 - X(\mathbf{8})]$ vs time for the reaction (phen)Pd(CH_3)(CO)$^+$ (**2**) + CO → (phen)Pd(C(O)CH_3)(CO)$^+$ (**8**) at −66 °C.

The reaction of (phen)Pd(CH_3)(^{12}CO)$^+$ with ^{13}CO was originally studied as a non-kinetic test of the migratory insertion mechanism. A solution of **2** was purged briefly with ^{13}CO at −78 °C. Incorporation of ^{13}CO into all of the available sites

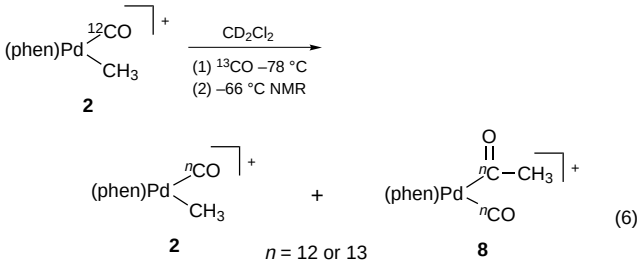

(6)

was observed in the −66 °C ^{1}H and ^{13}C NMR spectra. A crossover experiment was undertaken at −66 °C to determine if the label scrambling was the result of an associative or dissociative exchange. Complex **2*** and (bipy)Pd(CH_3)(CO)$^+$ (**12**) were combined and dissolved in CD_2Cl_2. No crossover was observed after 4 h at −66 °C; the ^{13}CO ligand remained in **2** (δ 175.9) and was not transferred into the terminal position of the bipyridine complex (δ 175.7). This negative crossover experiment indicates that in the experiment described by eq 6, a rapid *associative* exchange of free and coordinated CO, is occurring in addition to CO trapping of the unsaturated

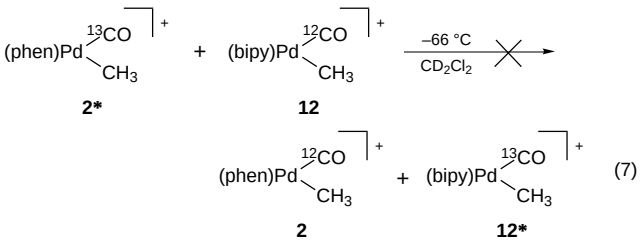

(7)

intermediate **2-I**.[46] Label scrambling of ^{12}CO into (*S*,*S*-BDPP)-Pd(CH_3)(^{13}CO)$^+BF_4^-$, has been described by Tòth and Elsevier, but no crossover experiment was reported.[29]

(d) Reaction of (phen)Pd(CH_3)(CO)$^+$ (2) with Acetone-d_6. Many carbonyl alkyl migratory insertion reactions display large rate enhancements in polar coordinating solvents.[6] The effect of acetone as a solvent was of particular interest because of the large number of keto groups present in the copolymer being formed. If there is a large rate enhancement upon CO insertion in acetone, this effect may also manifest itself during the copolymerization.

When complex **2** was dissolved in acetone-d_6, a temperature dependent equilibrium between **2** and a solvated acyl complex,

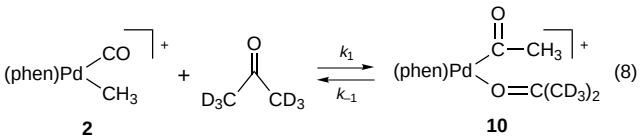

(8)

(phen)Pd(C(O)CH_3)(acetone-d_6)$^+$ (**10**), was observed.[44] The Pd−**C**(O)CH_3 carbonyl resonance occurs at δ 224.6, shifted *ca.* 8 ppm downfield from the analogous resonance in (phen)Pd(C(O)CH_3)(CO)$^+$, δ 216.5 (−58 °C). The methyl group displays a singlet at δ 2.57 in the ^{1}H NMR spectrum. This equilibrium was studied over a 63 deg temperature range; the thermodynamic parameters were evaluated from a van't Hoff plot, $\Delta H° = -4.1 \pm 0.15$ kcal/mol, $\Delta S° = -22 \pm 0.6$ eu.

The temperature dependence of the equilibrium constant allowed the forward and reverse rate constants for the equilibrium to be obtained using the "temperature-jump" method. The sample was warmed to *ca.* 40 °C to give a large population of **2** ($K_{40°C}$ (calc) = ca. 7×10^{-3} M) and placed in a −65 °C probe where the approach to equilibrium ($K_{-65°C} = 0.24 \pm 0.02$ M^{-1}) was observed. The rate at which equilibrium is attained is the sum of the forward and reverse rate constants (pseudo-first-order concentration of acetone-d_6 = 13.60 M); $k_1 + (k_{-1}/[\text{acetone-}d_6])$ is obtained as the slope of the plot of $-\ln[([\mathbf{10}]_t - [\mathbf{10}]_\infty)/([\mathbf{10}]_0 - [\mathbf{10}]_\infty)]$ versus time (Figure 6). Substitution into $K_{eq}[\text{acetone-}d_6] = k_1/(k_{-1}/[\text{acetone-}d_6])$ yields the rate constants $k_1 = (5.5 \pm 0.8) \times 10^{-4}$ s^{-1}, $\Delta G^‡_1 = 15.15 \pm 0.1$ kcal/mol and $(k_{-1}/[\text{acetone-}d_6]) = (1.8 \pm 0.4) \times 10^{-4}$ s^{-1}, $\Delta G^‡_{-1} = 15.6 \pm 0.1$ kcal/mol.[47] Assuming that the migratory insertion rate is in the saturation limit, there is only a *ca.* 2.5 fold increase in rate at −66 °C upon changing solvents from CD_2Cl_2 to acetone-d_6. This suggests that pendant ketone groups

(46) The displacement of CO in platinum square-planar complexes at high concentrations of trapping agent has also been shown to compete with insertion: Anderson, G. K.; Cross, R. J. *Acc. Chem. Res.* **1984**, *17*, 67.

(47) Two additional species were observed at constant concentration in solution while equilibrium was reattained. These were the carbonyl acetyl complex **10** (6.5%) and (phen)Pd(CH_3)(acetone-d_6)$^+$ (**13**) (4%). Complexes **10** and **13** must have formed at a higher temperature, since their concentrations are constant at −66 °C while those of **2** and **12** change with time.

(48) In the communication of this work,[21] the uncertainties in $\Delta H°$ (±0.5 kcal/mol) and $\Delta S°$ (±5 eu) were overestimated. Errors reported here were determined from a least squares analysis as described in the Experimental Section.

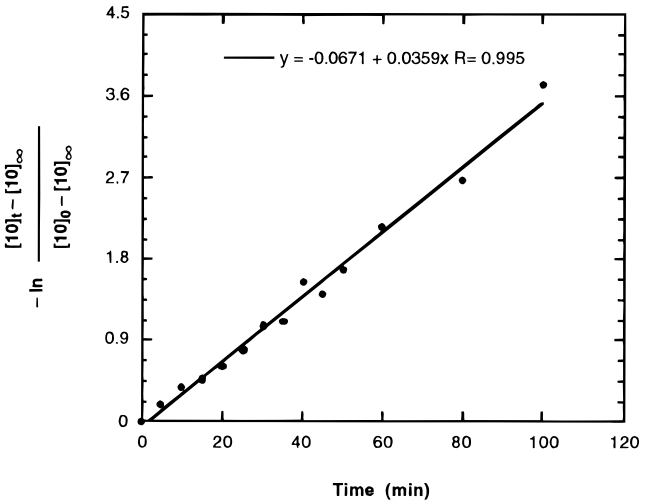

Figure 6. Representative plot of $-\ln[([\mathbf{10}]_t - [\mathbf{10}]_\infty)/([\mathbf{10}]_0 - [\mathbf{10}]_\infty)]$ vs time for the reaction (phen)Pd$(CH_3)(CO)^+$ (**2**) + acetone-d_6 $\rightleftharpoons$ (phen)Pd$(C(O)CH_3)$(acetone-d_6) (**10**) proceeding toward equilibrium at −65 °C.

Scheme 3. Reaction Products of (phen)Pd$(CH_3)(CO)^+$ (**2**) plus Ethylene[a]

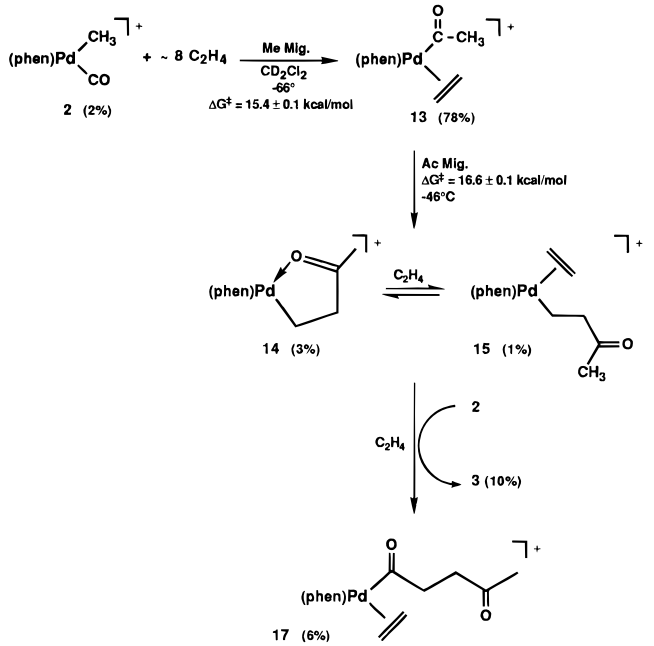

[a] Percentages shown in parentheses are the relative amounts of products after 98% conversion of **2** at −66 °C.

in the polymer should result in little acceleration of CO insertion and free energies of activation should remain at approximately 15 kcal/mol. (See Section 3e for additional details.)

(e) Reaction of (phen)Pd$(CH_3)(CO)^+$ (2) with C_2H_4. The β-acyl migration to ethylene is the second chain propagation step of the copolymerization. Therefore, an important target of our studies was to prepare the ethylene acetyl complex, (phen)Pd$(C(O)CH_3)(C_2H_4)^+$ (**13**), and examine its migratory insertion behavior. Reaction of **2** with ethylene (*ca.* 8 equiv) gives complex **13** (78%) as well as products arising from the subsequent acetyl migration reaction: **14** + **15** (total 4%) and (phen)Pd$(C(O)CH_2CH_2C(O)Me)(C_2H_4)^+$ (**17**) (6%) after 98% consumption of **2** (Scheme 3). The rate of conversion of **2** to **13** using ethylene as a trapping ligand $\{k = (2.2 \pm 0.1) \times 10^{-4}$ s^{-1}, $\Delta G^{\ddagger} = 15.4 \pm 0.1$ kcal/mol, saturation kinetics apply$\}$ is equivalent to that determined using CO as the trap. Since conversion of **2** to **13** is only slightly faster than migratory insertion of **13**, complete conversion of **2** results in some production of **14**, **15**, and **17** at −66 °C. Complex **17** incorporates two equiv of CO and thus **3** (*ca.* 10%) appears as the required non-CO containing Pd complex.

Ethylene-free solutions of **13** were obtained by holding the solution under vacuum at −78 °C for 15 h. Key spectroscopic data for **13**, obtained under these conditions, include broad coordinated ethylene resonances at δ 5.25 in the ^{1}H spectrum (−100 °C) and at δ 94 ($J_{CH} = 165 \pm 5$ Hz, $W_{1/2} = 35$ Hz, −100 °C) in the ^{13}C NMR spectrum. The ^{1}H resonance of coordinated ethylene remains a singlet at −120 °C. These chemical shifts are similar to those observed in **3** and **9**. The carbonyl carbon of the acetyl group absorbs at δ 223.0, comparable to the acetyl carbonyl of (phen)Pd$(C(O)CH_3)$-(acetone-$d_6)^+$ (δ 224.6).

Ethylene-catalyzed scrambling of the CO into the available coordination sites is occurring during the formation of **13**. The most obvious evidence for this is the appearance of **3** and **17** after 1 half-life of the reaction. It is also revealed in the dynamic behavior of the NMR spectra during the reaction. The equilibria K_1 and K_2 are attained on the NMR time scale as evidenced by the broadened methyl resonances of **2** and **3** and the averaged methyl resonances of **8** and **13**. The acetyl resonance represents the population weighted average of **8** (δ 2.916) and **13** (δ 2.729). This averaged resonance exhibits a small but constant change in chemical shift from 2.804 to 2.747 ppm as CO insertion proceeds during the first 1.7 half-lives of the disappearance of **2**. Since complexes **8** and **13** interconvert more rapidly than the rate of migratory insertion of **2**, eq 10 is driven to the right and 11 is driven to the left as the migratory insertion (eq 9) proceeds. This decreases the ratio of **8**/**13** with time, causing the averaged resonance to move upfield toward **13** (δ 2.729) as the reaction proceeds to completion.

$$\underset{\mathbf{2}}{(\text{phen})\text{Pd}(CH_3)(CO)^+} + C_2H_4 \xrightarrow{k} \underset{\mathbf{13}}{(\text{phen})\text{Pd}(C(O)CH_3)(C_2H_4)^+} \quad (9)$$

$$\underset{\mathbf{2}}{(\text{phen})\text{Pd}(CH_3)(CO)^+} + C_2H_4 \overset{K_1}{\rightleftharpoons} \underset{\mathbf{3}}{(\text{phen})\text{Pd}(CH_3)(C_2H_4)^+} + CO \quad (10)$$

$$\underset{\mathbf{13}}{(\text{phen})\text{Pd}(C(O)CH_3)(C_2H_4)^+} + CO \overset{K_2^{-1}}{\rightleftharpoons} \underset{\mathbf{8}}{(\text{phen})\text{Pd}(C(O)CH_3)(CO)^+} + C_2H_4 \quad (11)$$

The combination of eqs 9, 10, and 11 would convert **2** completely to **13**. However, **16**, one of the products of the migratory insertion of **13**, undergoes a second CO insertion (eqs 12 and 13) requiring that an equal concentration of **3** be formed.

$$\underset{\mathbf{14}}{(\text{phen})\text{Pd}(CH_2CH_2C(O)CH_3)^+} + CO \rightleftharpoons \underset{\mathbf{16}}{[(\text{phen})\text{Pd}(CH_2CH_2C(O)CH_3)(CO)^+]} \quad (12)$$

$$\mathbf{16} + C_2H_4 \rightarrow \underset{\mathbf{17}}{(\text{phen})\text{Pd}(C(O)CH_2CH_2C(O)CH_3)(C_2H_4)^+} \quad (13)$$

Even though the concentrations of **2**, **3**, **8**, **13**, and ethylene were known, absolute equilibrium constants K_1 and K_2 could not be

determined because [CO] was too low to be accurately measured by conservation of mass calculations. This reinforces the premise that while CO may rapidly exchange with ethylene, CO is still the thermodynamically favored ligand.

Nevertheless, the ratio of the two equilibrium constants, K_2/K_1, can be obtained. The concentrations of ethylene and CO may be factored out of the full expression of K_2/K_1 since they are constant in the system at any one time:

$$K_2/K_1 = ([\mathbf{13}][\mathrm{CO}]/[\mathbf{8}][\mathrm{C_2H_4}])/([\mathbf{3}][\mathrm{CO}]/[\mathbf{2}][\mathrm{C_2H_4}])$$

$$K_2/K_1 = ([\mathbf{13}]/[\mathbf{8}])/([\mathbf{3}]/[\mathbf{2}])$$

Substitution of the relative amounts of **2**, **3**, **8**, and **13** (determined during the second half-life of the reaction when **3** was directly observable) yields $K_2/K_1 = 34 \pm 4$. The terminal ν_{CO} of **2** and **8** only differ by 2 cm^{-1}, indicating that the metal centers are similar electronically. Since CO is a smaller ligand than ethylene, the fact that K_2 is greater than K_1 probably reflects less steric repulsion between ethylene and the trigonal acyl ligand relative to the tetrahedral methyl group. The preference for ethylene binding to the acetyl complex explains why **13** forms at the limiting rate observed in the other trapping experiments during the first half-life. At early time, there is little (phen)Pd(C(O)CH_3)(CO)$^+$ and (phen)Pd(Me)(C_2H_4)$^+$ present and a rate-decreasing preequilibrium between **2**, **3**, **8**, and **13** is not significant.

The MA trapping study of the migratory insertion reaction of **2** is unaffected by CO scrambling because MA binds much weaker than CO to Pd and the product of migratory insertion, (phen)Pd(CH(CO_2CH_3)CH_2C(O)CH_3), does not react with CO under the experimental conditions. Thus, CO remains coordinated in **2** and CO scrambling is not observed during these saturation kinetics experiments.

Migration of the acetyl group to ethylene in complex **13** was observed *in situ* by ^{1}H NMR spectroscopy at −46 °C. In the presence of ethylene, **13** yields an equilibrating pair of complexes, the 5-membered chelate **14**, and its ethylene coordinated open form **15**. The first-order rate constant for acetyl migration in the presence of either 7 or 14 equiv of ethylene was $k_{Ac\rightarrow C_2H_4} = (4.8 \pm 0.4) \times 10^{-4}$ s^{-1} and $\Delta G^{\ddagger}_{Ac\rightarrow C_2H_4} = 16.6 \pm 0.1$ kcal/mol (−46 °C). In the absence of free ethylene, the rearrangement of **13** to **14** occurs at the same rate, $k = 4.7 \times 10^{-4}$ s^{-1} (−46 °C).

The chelate **14** was independently prepared by the addition of ethylene to **2** at 20 °C followed by crystallization from CH_2Cl_2. Subsequent exposure of **14** to ethylene confirmed generation of an equilibrating mixture of **14** and **15**. The temperature dependent equilibrium, **14** + C_2H_4 ⇌ **15**, was studied in CD_2Cl_2 from −92 to −57 °C, giving $\Delta H° = -7.8 \pm 0.3$ kcal/mol

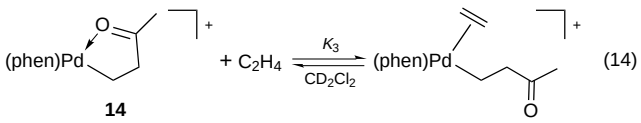

(14)

and $\Delta S° = -36 \pm 1.5$ eu.[48] The transient presence of the CO coordinated analogue of **15**, (phen)Pd($CH_2CH_2C(O)CH_3$)(CO)$^+$ (**16**) (Scheme 4), is evidenced by the formation of a new acyl species identified as (phen)Pd(C(O)$CH_2CH_2C(O)CH_3$)(C_2H_4)$^+$ (**17**). Since **17** is such a minor product, the presence of the CO coordinated analogue of **17**, (phen)Pd(C(O)$CH_2CH_2C(O)CH_3$)(CO)$^+$ (**18**), was not observed.

Scheme 4. *In Situ* Generation of (phen)Pd($CH_2CH_2C(O)CH_3$)(CO)$^+$ (**16**)[a]

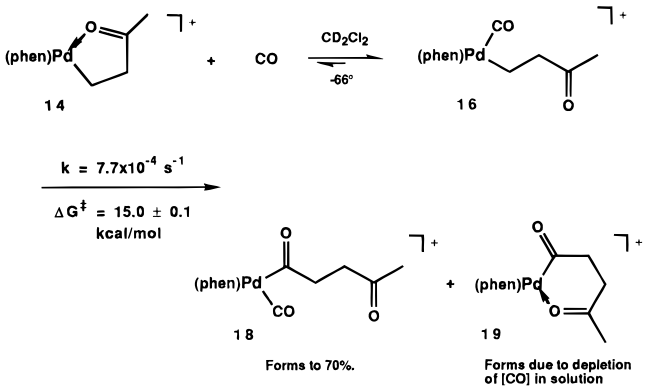

[a] Alkyl migration to CO, and trapping by CO or γ-acetyl forms **18** and **19**, respectively. Complex **19** forms after the CO in solution is consumed.

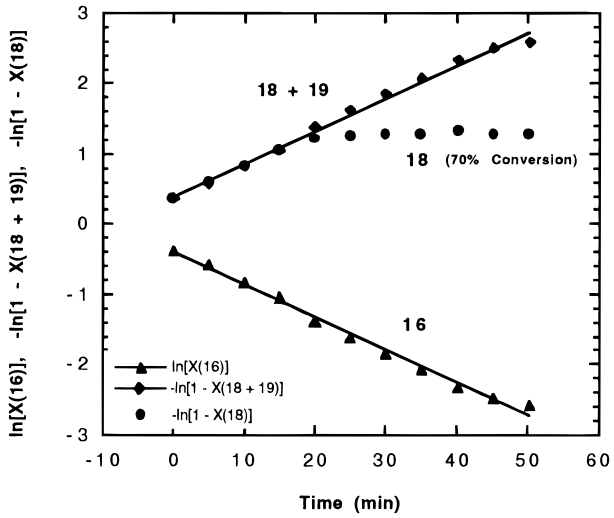

Figure 7. Natural log plot of mole fraction (X) versus time for the reaction of (phen)Pd($CH_2CH_2C(O)CH_3$)(CO)$^+$ (**16**) + CO at −66 °C. The first product observed is the carbonyl acyl (phen)Pd(C(O)CH_2-CH_2C(O)CH_3)(CO)$^+$ (**18**); when CO in solution is consumed, the 6-membered chelate (phen)Pd(C(O)CH_2CH_2C(O)CH_3)$^+$ (**19**) forms at the same saturation rate as CO trapping to form **18**, $k = 7.7 \times 10^{-4}$ s^{-1}, $\Delta G^{\ddagger} = 15.0 \pm 0.1$ kcal/mol.

The carbonyl alkyl intermediate (phen)Pd($CH_2CH_2C(O)CH_3$)-(CO)$^+$ (**16**) has been prepared *in situ*, in a similar manner to **15**, by exposure of **14** to CO at −78 °C. In the presence of excess CO, **16** gives the carbonyl acyl complex (phen)Pd(C(O)-$CH_2CH_2C(O)CH_3$)(CO)$^+$ (**18**) as the main product. However, as in the conversion of (phen)Pd(CH_3)(CO)$^+$ to (phen)Pd(C(O)-CH_3)(CO)$^+$, the limitation of low [CO] could be observed. In the present case, the concentration of starting material did not level off; *instead*, complex **19** formed from the γ-keto group acting as the trapping ligand. A similar 6-membered norbornyl chelate has been observed by Elsevier and co-workers.[35] The linearity of the natural log plot for formation of the sum **18** + **19** indicates that the migratory insertion and ligand (CO and γ-keto) trapping occurs in the saturation limit of the steady state analysis.

We measured the rate of the transformation of **16** to **19** in the absence of CO in solution in order to verify that the rates of trapping by the γ-acetyl group and CO are the same. Complex **16** was formed from **14** and CO, and the CO in

Scheme 5. Generation of (phen)Pd($CH_2CH_2C(O)CH_3$)$(CO)^+$ in the Absence of External CO[a]

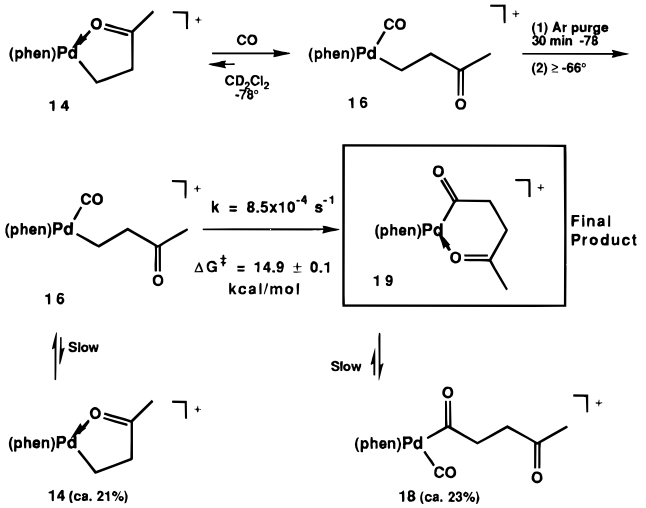

[a] Unreacted complexes **14** and **18**, at −66 °C, completely yield **19** upon warming to −25 °C.

solution was removed by an argon purge at −78 °C for 30 min (Scheme 5). It was surprising to observe in the −66 °C ^{1}H NMR spectrum a mixture of **14** (24%), **16** (23%), **19** (30%), and **18** (23%). The formation of complexes **14** and **18** must occur either during the purge with argon or *en route* to the cold NMR probe, because their concentrations vary little while **16** rearranges to **19**. The rearrangement was followed for 3 half-lives: $k = 8.5 \times 10^{-4}$ s^{-1}, $\Delta G^{\ddagger} = 14.9 \pm 0.1$ kcal/mol (−66 °C). The barrier for this rearrangement is the same observed for the formation of **18** + **19** from **16** in the presence of CO. The complete conversion of **14** and **18** into **19** is accomplished by warming the sample to −25 °C.

The *in situ* synthesis of the 6-membered chelate, **19**, has allowed the ethylene acyl complex **17**, (phen)Pd($C(O)CH_2$-$CH_2C(O)CH_3$)$(C_2H_4)^+$, to be prepared (Scheme 6). As with the interconversion of **14** + ethylene ⇌ **15**, there is a temperature-dependent equilibrium between **19** plus ethylene and its ethylene coordinated open form **17**. In the presence of *ca.* 9 equiv of ethylene, this equilibrium is attained on the fast-exchange limit of the NMR time scale at *ca.* −65 °C. The equilibrium constants, determined from −63.8 to −44.4 °C, were evaluated from the population weighted averaged chemical shift of the ^{13}C-labeled terminal carbonyl moiety of (phen)Pd($C(O)CH_2CH_2{}^{13}C(O)CH_3$)$(C_2H_4)^+$ (δ 207.7) and (phen)Pd($\overline{C(O)CH_2CH_2{}^{13}C(O)CH_3}$)$^+$ (δ 222.1) (^{13}C, 75.4 MHz, $\Delta\nu = 1086$ Hz); [ethylene] was determined from the ^{1}H NMR spectra. A van't Hoff plot yielded $\Delta H° = -6.5 \pm 1.1$ kcal/mol and $\Delta S° = -24 \pm 5$ eu. Comparison of the thermodynamic parameters for the opening of the 5- and 6-membered chelates **14** ($\Delta H° = -7.8 \pm 0.3$ kcal/mol, $\Delta S° = -36 \pm 1.5$ eu) and **19** ($\Delta H° = -6.5 \pm 1.1$ kcal/mol, $\Delta S° = -24 \pm 5$ eu) reveals that opening of the 6-membered chelate at −44 °C is slightly favored due to its less negative $\Delta S°$.

We sought to measure the rate of β-acyl migratory insertion of **17** because the $-C(O)CH_2CH_2C(O)CH_3$ group closely mimics a pendant polymer chain. The transformation of the pair of **19*** and **17*** into the rapidly interconverting pair of **20** and **21**, one repeat unit analogs of **14** and **15**, was followed by ^{1}H NMR spectroscopy at −44.4 °C. The rate of β-acyl migration was extracted from the rate of decay of the averaged methyl resonances of **19*** and **17***. A plot of ln([**19***] + [**17***])

Scheme 6. Measurement of the Preequilibrium between **19*** + Ethylene and **17*** and the Subsequent β-Acyl Migratory Insertion

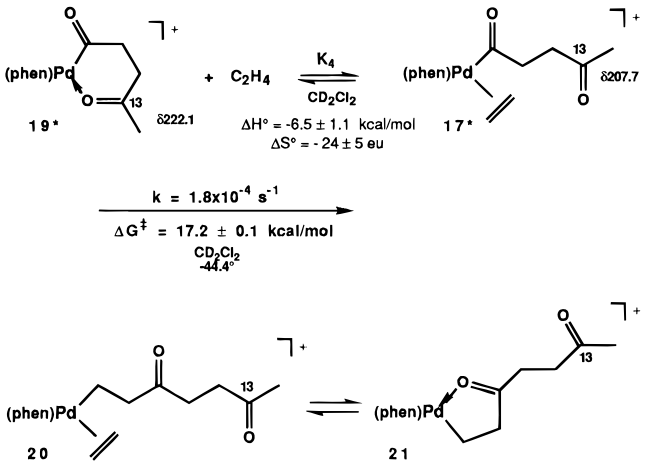

versus time gives

$$k_{obs} = -k(K_{eq}[C_2H_4]/(1 + K_{eq}[C_2H_4]))$$

Upon substitution of $K_{eq} = 10.5$ L/mol and [ethylene] = 0.1275 M (ca. 8.5 equiv) the rate constant for migratory insertion is obtained: $k = 1.8 \times 10^{-4}$ s^{-1}, $\Delta G^{\ddagger} = 17.2 \pm 0.1$ kcal/mol.

4. Mechanistic Model for the Copolymerization of Ethylene with CO. (a) Relative Binding Affinities of CO and C_2H_4 to Palladium. At this point, the barriers to migratory insertion for models of the propagation steps (eqs 15 and 16) have been determined and the temperature dependent equilibria of the chelate complexes **14** and **19** and their respective ethylene coordinated open forms **15** and **17** have been characterized (eqs 17 and 18):

$$\underset{\mathbf{16}}{(\text{phen})\text{Pd}(CH_2CH_2C(O)CH_3)(CO)^+} + CO \xrightarrow[\Delta G^{\ddagger} = 15.0 \text{ kcal/mol}]{} \mathbf{18} + \mathbf{19} \quad (15)$$

$$\underset{\mathbf{17}}{(\text{phen})\text{Pd}(C(O)CH_2CH_2C(O)CH_3)(C_2H_4)^+} + C_2H_4 \xrightarrow[\Delta G^{\ddagger} = 17.2 \text{ kcal/mol}]{} \mathbf{20} + \mathbf{21} \quad (16)$$

$$\underset{\mathbf{14}}{(\text{phen})\text{Pd}(\overline{CH_2CH_2C(O)}CH_3)^+} + C_2H_4 \rightleftharpoons \underset{\mathbf{15}}{(\text{phen})\text{Pd}(CH_2CH_2C(O)CH_3)(C_2H_4)^+} \quad (17)$$

$\Delta H° = -7.8 \pm 0.3$ kcal/mol, $\Delta S° = -36 \pm 1.5$ eu

$$\underset{\mathbf{19}}{(\text{phen})\text{Pd}(\overline{C(O)CH_2CH_2C(O)}CH_3)^+} + C_2H_4 \rightleftharpoons \underset{\mathbf{17}}{(\text{phen})\text{Pd}(C(O)CH_2CH_2C(O)CH_3)(C_2H_4)^+} \quad (18)$$

$\Delta H° = -6.5 \pm 1.1$ kcal/mol, $\Delta S° = -24 \pm 5$ eu

The remaining information necessary to construct a working mechanistic model for the copolymerization is the relative binding affinities of CO and ethylene to these palladium

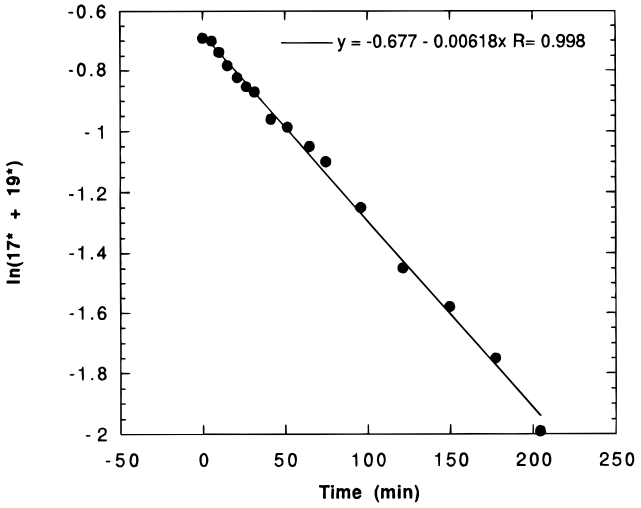

Figure 8. Plot of ln([**19***] + [**17***]) versus time.

complexes:

$$(\text{phen})\text{Pd}(\text{C(O)CH}_2\text{CH}_2\text{C(O)CH}_3)(\text{CO})^+ + \text{C}_2\text{H}_4 \overset{K_5 = ?}{\rightleftharpoons} \underset{\mathbf{18}}{} \quad (\text{phen})\text{Pd}(\text{C(O)CH}_2\text{CH}_2\text{C(O)CH}_3)(\text{C}_2\text{H}_4)^+ + \text{CO} \quad (19)$$
$$\mathbf{17}$$

$$(\text{phen})\text{Pd}(\text{CH}_2\text{CH}_2\text{C(O)CH}_3)(\text{CO})^+ + \text{C}_2\text{H}_4 \overset{K_6 = ?}{\rightleftharpoons} \underset{\mathbf{16}}{} \quad (\text{phen})\text{Pd}(\text{CH}_2\text{CH}_2\text{C(O)CH}_3)(\text{C}_2\text{H}_4)^+ + \text{CO} \quad (20)$$
$$\mathbf{15}$$

The complexes (phen)Pd(C(O)CH_2CH_2C(O)CH_3)(L)$^+$ (L = C_2H_4, CO) and (phen)Pd(CH_2CH_2C(O)CH_3)(L)$^+$ (L = C_2H_4, CO) are excellent models for active catalysts responsible for chain growth. They effectively contain three and two repeat units tethered to palladium. After K_5 and K_6 are obtained, they can be combined with the known barriers to migratory insertion for **16** and **17** to produce a mechanistic model of copolymer chain growth.

The strategy that we employed to find K_5 and K_6 was to first measure relative equilibrium constants K_5/K_1 and K_6/K_1, then determine K_1 (eq 10) independently through a series of pairwise ligand binding studies. Once K_5 and K_6 are determined, the importance of the chelate complexes in the catalytic cycle can also be assessed. The experiments devised to measure K_5/K_1 and K_6/K_1 are very similar to those used for evaluation of K_2/K_1 (Section 2). The general approach involved combining the carbonyl methyl complex, **2**, with the 5- or 6-membered chelated, **14** or **19***, in CD_2Cl_2, adding ethylene, and observing the relative amounts of the ethylene and CO coordinated products. For determining K_5/K_1, a solution of **2** was added to a separate solution of **19*** (prepared *in situ* from **14***) at −78 °C then ethylene was added. Ethylene catalyzed the scrambling of CO between all of the available sites forming a mixture of **2**, **3**, **17***, and **18*** (Scheme 7). A ^{13}C-labeled acetyl carbonyl was observed at δ 208, indicating that **19*** (δ 222.1) was not present in significant amounts. The integrals of **2** and **3** in the ^{1}H NMR (−83 °C) spectrum could be evaluated directly while the resonances for **17*** and **18*** were averaged. However, as in the reaction of **2** with ethylene, there is very little free CO present; the approximation that the amount of CO lost by **2** is being retained by **18*** (that is [**18***] = [**3**]) can be made. The

Scheme 7. Determining K_5/K_1 from the Reaction of **19*** + **2** + C_2H_4[a]

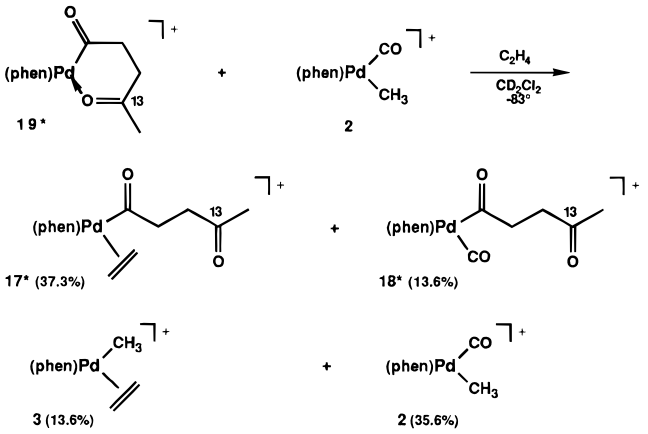

[a] K_5/K_1 = ([**17***]/[**18***])/([**3**]/[**2**]) = 7.2.

Scheme 8. Determining K_6/K_1 from the Reaction of **14** + **2** + Ethylene at −66 °C[a]

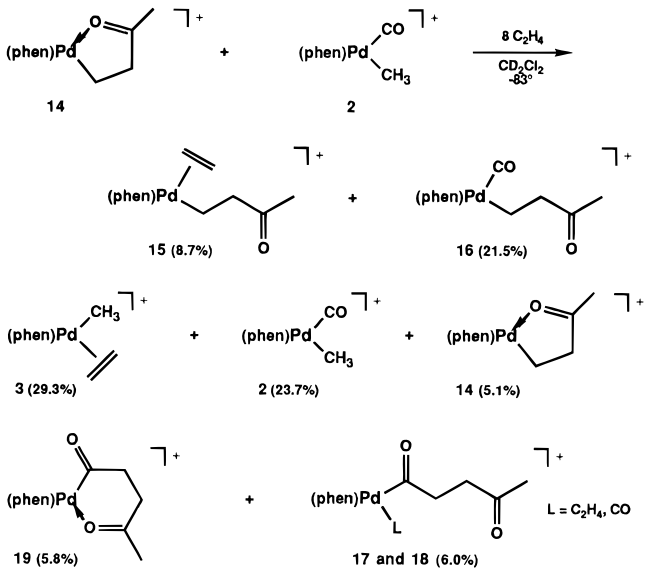

[a] K_6/K_1 = ([**15**]/[**16**])/([**3**]/[**2**]) = 0.33.

K_5/K_1 ratio can then be evaluated:

$$K_5/K_1 = ([\mathbf{17}^*]/[\mathbf{18}^*])/([\mathbf{3}]/[\mathbf{2}])$$

$$K_5/K_1 = (37.3/13.6)/(13.6/35.6) = 7.2$$

This factor is smaller than that observed for K_2/K_1 (acetyl vs methyl) by a factor of *ca.* 5 and reflects the fact that −C(O)CH_2CH_2C(O)CH_3 is more sterically demanding than −C(O)CH_3.

The ratio of K_6/K_1 was determined in a similar manner. Ethylene was added to a solution of **2** and **14** at −78 °C (Scheme 8). Scrambling of CO and ethylene was observed in the −83 °C ^{1}H NMR spectrum; the integrals of **2**, **3**, **15** and **16** were determined independently giving

$$K_6/K_1 = ([\mathbf{15}]/[\mathbf{16}])/([\mathbf{3}]/[\mathbf{2}])$$

$$K_6/K_1 = (8.7/21.5)/(29.3/23.7) = 0.33$$

The factor of 0.33 reflects the larger steric bulk of −CH_2CH_2C(O)CH_3 compared to −CH_3 as seen by ethylene, relative to CO, in the two alkyl complexes. A mass balance analysis of the seven palladium species in solution revealed that only a small amount of CO (ca. 7%), initially from **2**, is unaccounted for.

Table 2. Equilibrium Constants at −66 °C for (phen)Pd(CH_3)(L)$^+$ + L′ = (phen)Pd(CH_3)(L′)$^+$ + L

L =	L′ =	equilibrium	K (−66 °C)	$\Delta G°$ [a]
CO	MeSPh	K_A[b]	$(7.66 \pm 3.45) \times 10^{-4}$	3.0 ± 0.2
MeSPh	CH_3CN	K_B	$(6.81 \pm 0.27) \times 10^{-3}$	2.05 ± 0.02
CH_3CN	$H_2C{=}CH_2$	K_C[c]	$(8.58 \pm 1.8) \times 10^{-1}$	0.07 ± 0.09
C_6H_5CN	$H_2C{=}CH_2$	K_D	1.56 ± 0.13	-0.18 ± 0.04
CH_3CN	C_6H_5CN	K_E	$(5.5 \pm 0.7) \times 10^{-1}$	0.25 ± 0.05
CO	$H_2C{=}CH_2$	K_1[d]	$(4.48 \pm 3.14) \times 10^{-6}$	5.12 ± 0.31

[a] $\Delta G°$ was calculated as the average of the high and low values of K_{eq}. [b] The equilibrium constant K_A was measured at −83 °C ($(3.8 \pm 1.6) \times 10^{-4}$) and extrapolated to −66 °C from $\Delta G°_A$. [c] K_C was calculated from $K_D K_E$. [d] K_1 was calculated from $K_A K_B K_C$ and then $\Delta G°_1$ was calculated from K_1.

This validates the previous approximation that the CO lost from **2** is taken up in **18*** in the K_5/K_1 calculation.

(b) Determining the Absolute Equilibrium Constants K_1, K_5, and K_6. The equilibrium constant, K_1, for competitive ethylene and CO binding to (phen)Pd(CH_3)$^+$ (eq 21) is too large

$$\underset{\mathbf{2}}{(\text{phen})\text{Pd}(CH_3)(CO)^+} + C_2H_4 \overset{K_1}{\rightleftharpoons} \underset{\mathbf{3}}{(\text{phen})\text{Pd}(CH_3)(C_2H_4)^+} + CO \quad (21)$$

to measure directly from the addition of ethylene to **2**. Thus the equilibrium constant must be determined in a stepwise fashion using ligands with binding affinities between that of CO and ethylene. The choice of these reactions is often tedious, but fortunately Kurosawa and co-workers tackled an almost identical problem for the series of cationic 18 e$^-$ complexes Cp(R_3P)Pd(L)$^+$.[49] The intermediate ligands that we chose, thioanisole and acetonitrile, were selected based on Kurosawa's studies. The relative ligand binding affinities are CO > S(CH_3)(C_6H_5) > CH_3CN ∼ ethylene > C_6H_5CN. Equilibrium constants and $\Delta G°$ values evaluated at −66 °C are listed in Table 2.

The equilibrium constant for the reaction of **2** with thioanisole was measured at −83 °C. A solution of **2** was saturated with CO at −78 °C, thioanisole was added, and after calculating the concentration of CO ([CO] = 7.0×10^{-3} M) using Bryndza's equation,[50] K_A was determined to be $(3.8 \pm 1.6) \times 10^{-4}$ at −83 °C.

$$\underset{\mathbf{2}}{(\text{phen})\text{Pd}(CH_3)(CO)^+} + CH_3SC_6H_5 \overset{K_A}{\rightleftharpoons} \underset{\mathbf{4}}{(\text{phen})\text{Pd}(CH_3)(CH_3SC_6H_5)^+} + CO \quad (22)$$

Thioanisole is a much better ligand than acetonitrile. In order to reduce the amount of error associated with evaluating the large difference between the integral of acetonitrile relative to

$$\underset{\mathbf{4}}{(\text{phen})\text{Pd}(CH_3)(CH_3SC_6H_5)^+} + NCCH_3 \overset{K_B}{\rightleftharpoons} \underset{\mathbf{5}}{(\text{phen})\text{Pd}(CH_3)(NCCH_3)^+} + CH_3SC_6H_5 \quad (23)$$

5, a CD_3CN solution of CH_3CN (11.7 mol % CH_3CN) was prepared and used to evaluate K_B ($(6.81 \pm 0.27) \times 10^{-3}$) at −66 °C.[51] The binding affinities of ethylene and nitriles such as CH_3CN and C_6H_5CN are similar, and the equilibrium constant

Table 3. Equilibrium Constants and $\Delta G°$ for the Equilibria of the Mechanistic Model

equilibrium (T)	$K(T)$	$\Delta G°(T)$[a]	K (25 °C)[b]
K_1(−66°C)	$(4.48 \pm 3.14) \times 10^{-6}$	5.12 ± 0.31	$(2.0 \pm 1) \times 10^{-4}$
K_2(−66°C)	$(1.52 \pm 1.25) \times 10^{-4}$	3.85 ± 0.48	$(2.0 \pm 1) \times 10^{-3}$
K_3(25°C) (M^{-1})			$(5.7 \pm 1) \times 10^{-3}$
K_4(25°C) (M^{-1})			0.36 ± 0.3
K_5(−83°C)[c,d]	$(1.27 \pm 0.85) \times 10^{-5}$	4.37 ± 0.31	$(7.1 \pm 3.5) \times 10^{-4}$
K_6(−83°C)[c,e]	$(5.84 \pm 3.93) \times 10^{-7}$	5.54 ± 0.31	$(9.9 \pm 5) \times 10^{-5}$
K_5/K_4(25°C) (M)			$(2.0 \pm 2) \times 10^{-3}$
K_6/K_3(25°C) (M)			$(1.7 \pm 1) \times 10^{-2}$

[a] In units of kcal/mol. [b] K(25°C) extrapolated from $\Delta G°$ except for K_3 and K_4 which were extrapolated from van't Hoff plots (Tables 5, 8). [c] $K_1(-83°C) = (1.77 \pm 1.19) \times 10^{-6}$. [d] $K_5/K_1(-83°C) = 7.2$. [e] $K_6/K_1(-83°C) = 0.33$.

K_C was calculated as $(8.58 \pm 1.8) \times 10^{-1}$ at −66 °C (Table 2).

$$\underset{\mathbf{5}}{(\text{phen})\text{Pd}(CH_3)(NCCH_3)^+} + C_2H_4 \overset{K_c}{\rightleftharpoons} \underset{\mathbf{3}}{(\text{phen})\text{Pd}(CH_3)(C_2H_4)^+} + NCCH_3 \quad (24)$$

After extrapolating K_A to −66 °C, from $\Delta G°_A$, the product of the three equilibrium constants, $K_A K_B K_C$, yields $K_1 = (4.48 \pm 3.14) \times 10^{-6}$ and $\Delta G°_1 = 5.12 \pm 0.31$ kcal/mol at −66 °C. The equilibrium constants K_5 and K_6 can now be calculated from K_5/K_1 and K_6/K_1 after extrapolation of K_1 to −83 °C, the temperature at which K_6/K_1 and K_5/K_1 were measured: K_5(−83°C) = $(1.27 \pm 0.85) \times 10^{-5}$; K_6 (−83°C) = $(5.84 \pm 3.93) \times 10^{-7}$. A complete list of the equilibrium constants is given in Tables 2 and 3.

(c) Mechanistic Model for Copolymer Chain Growth. Now that the kinetic and thermodynamic data have been secured, a mechanistic model of copolymer chain growth can be constructed. Scheme 9 shows the working model with values of K_{eq} and k_{ins} extrapolated from $\Delta G°$ and $\Delta G^‡$, assuming that the entropy contributions are negligible. This is a fair assumption considering that migratory insertion reactions, being intramolecular, typically have $\Delta S^‡ \sim 0$ and $\Delta G^‡ \sim \Delta H^‡$ as seen for the β-ethyl migratory insertion of **7** ($\Delta S^‡ = -3.7 \pm 2.0$ eu).[10,16,17,52] The degrees of freedom and the solvation of (phen)Pd(R)(L)$^+$ should not change signigficantly upon substitution of ethylene and CO ligands. Also, the free ligands have similar standard entropies[53] ($\Delta S°$(CO) = 47.2 eu, $\Delta S°$-(C_2H_4) = 52.2 eu) and solvation entropies in halogenated solvents such as chlorobenzene[54] ($\Delta S°_{solv}$(CO) = −12.98 eu, $\Delta S°_{solv}(C_2H_4)$ = −16.10 eu), giving only a small (*ca.* 2 eu) overall entropy difference. Thus the assumptions $\Delta G^‡ = \Delta H^‡$ and $\Delta G° = \Delta H°$ are not unreasonable and suggest that extrapolations of the low-temperature data to room temperature can be made without introduction of unreasonably large errors.

Based on the thermodynamic and kinetic data shown in Scheme 9, it is clear that the carbonyl acyl intermediates, **18-P**, are the most stable species in the copolymerization cycle and are thus the catalyst resting state(s). This is consistent with previous spectroscopic observations in the *p-tert*-butylstyrene/CO copolymerization system.[22]

(49) Kurosawa, H.; Majima, T.; Asada, N. *J. Am. Chem. Soc.* **1980**, *102*, 6996.

(50) Bryndza, H. E. *Organometallics* **1985**, *4*, 1686.

(51) A thermodynamic isotope effect favoring binding of one of the isotopomers is expected to be negligible.

(52) The $\Delta S^‡$ for the carbonyl methyl insertion of (DPPP)Pd(CH_3)-(CO)$^+$Ar′$_4$B$^-$ is ca. 0 eu. Ledford, J. S.; Brookhart, M. Personal communication.

(53) Atkins, P. W. *Physical Chemistry*, 3rd ed.; W. H. Freeman and Company: New York, 1986.

(54) Wilhelm, E.; Battino, R. *Chem. Rev.* **1973**, *73*, 1.

Scheme 9. Complete Mechanistic Cycle of Chain Propagation for the Copolymerization of Ethylene with CO[a]

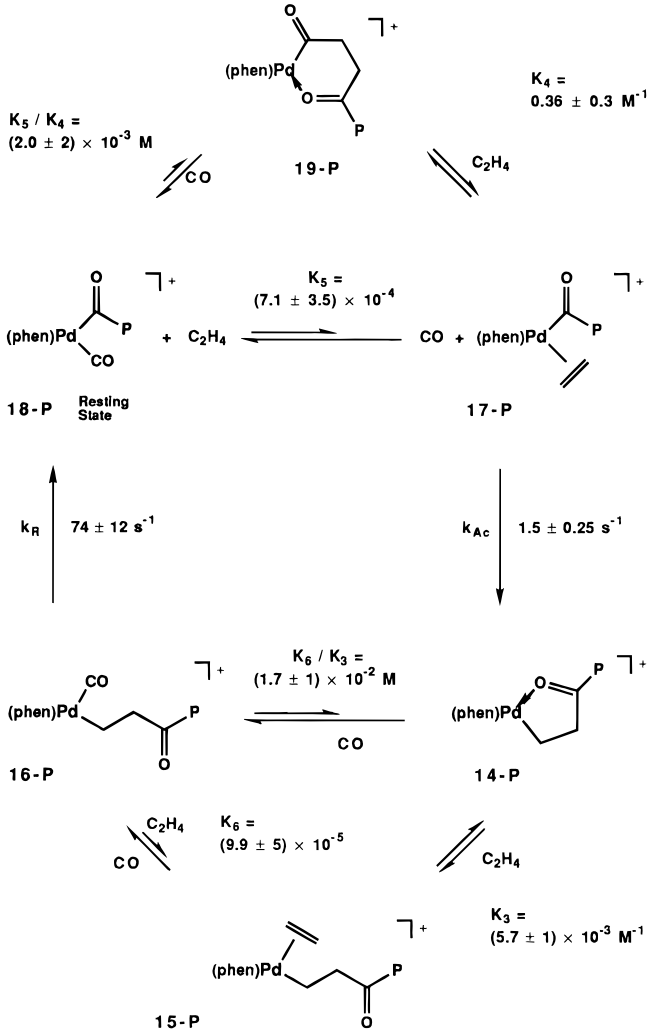

[a] Equilibrium and rate constants calculated at 25 °C.

This model predicts that the overall rate of chain growth is

$$\mathrm{d}(-\mathrm{C(O)CH_2CH_2}-)/\mathrm{d}t = K_5 k_{\mathrm{Ac}}[\mathrm{Pd}][\mathrm{C_2H_4}]/[\mathrm{CO}]$$

The turnover frequency is this rate normalized by [Pd], giving

$$\text{turnover frequency} = K_5 k_{\mathrm{Ac}}[\mathrm{C_2H_4}]/[\mathrm{CO}]$$

Corrections for the concentrations of species besides **18-P** are not necessary since they are very small. Substitution of $[C_2H_4] = 0.11 \pm 0.01$ M, $[CO] = 7.3 \times 10^{-3}$ M (at 1 atm of pressure of 1:1 ethylene/CO gas), and the extrapolated values for K_5 ($(7.1 \pm 3.5) \times 10^{-4}$) and k_{Ac} (1.5 ± 0.25) at 25 °C yield:

$$\text{turnover frequency (calc)} = ((7.1 \pm 3.5) \times 10^{-4})(1.5 \pm 0.25\ \mathrm{s^{-1}})(0.11 \pm 0.01\ \mathrm{M})/(7.3 \times 10^{-3}\ \mathrm{M}) = (16 \pm 12) \times 10^{-3}\ \mathrm{s^{-1}}$$

Wagner and Brookhart have measured the turnover frequency of the catalyst as 8×10^{-3} s^{-1}.[55] This value is in remarkably good agreement with the value predicted on the basis of our kinetic and thermodynamic measurements. As argued above, this agreement is likely resulted from values of $\Delta S^{\ddagger}$ (for k_{Ac}) and $\Delta S°$ (for K_5) being close to zero. Alternatively, $\Delta S^{\ddagger}$ and $\Delta S°$ could be larger than expected in magnitude but offsetting in sign, $\Delta S^{\ddagger} \approx -\Delta S°$. While further studies will be necessary to resolve this particular issue, the overall study still strongly supports the chain growth mechanism. Important features of the copolymerization that have been studied include the direct observation of the key carbonyl alkyl, ethylene acyl, and ethylene alkyl complexes and the determination of their migratory insertion aptitudes and also the measurement of the relative binding affinities of ethylene and CO to both alkyl and acyl palladium moieties. These studies reveal that the two factors resposible for enforcing the alternating nature of the copolymerization are (1) carbon monoxide binds much tighter than ethylene to palladium and (2) migratory insertions of carbonyl alkyl complexes are much more facile than those of ethylene alkyl complexes.

Table 4. Free Energies of Activation for the Migratory Insertion Reactions of $(phen)Pd(R)(L)^+$

R	L	$\Delta G^{\ddagger}$ (kcal/mol)[a]	temp (°C)
CH_3 (CD_2Cl_2)	CO	15.4	−66
CH_3 (acetone-d_6)	CO	15.15	−65
$CH_2CH_2C(O)CH_3$	CO	15.0	−66
$C(O)CH_3$	$CH_2{=}CH_2$	16.6	−46
$C(O)CH_2CH_2C(O)CH_3$	$CH_2{=}CH_2$	17.2	−44.4
CH_3	$CH_2{=}CH_2$	18.5	−25
CH_2CH_3	$CH_2{=}CH_2$	19.4	−25

[a] Errors of ±0.1 kcal/mol.

The kinetic and thermodynamic data also allow the fraction of mistakes due to consecutive ethylene insertions, that occur during the copolymerization, to be estimated. This ratio is equal to the relative rates of insertion of the carbonyl and ethylene alkyl complexes. Employing the rate constants for migratory insertion of **16** and **7** (as an estimate for that of **15** which is not possible to observe directly[56]), the equilibrium constant K_6, and the concentrations of [CO] and [ethylene], the expression

$$\begin{aligned}\text{ethylene insertion/CO insertion} &= k_{\mathrm{e}}[\mathbf{15}]/k_{\mathrm{CO}}[\mathbf{16}] \\ &= (k_{\mathrm{e}}/k_{\mathrm{CO}})K_6[\mathrm{C_2H_4}]/[\mathrm{CO}] \\ &= (0.037/74)(9.9 \times 10^{-5}) \times (0.11\ \mathrm{M})/(7.3 \times 10^{-3}\ \mathrm{M}) \\ &= 7.5 \times 10^{-7}\end{aligned}$$

can be evaluated. Consecutive ethylene insertions are thus expected to occur roughly $1/10^6$ times. This partitioning is primarily a result of the magnitude of K_6 (9.9×10^{-5}) favoring coordination of CO over ethylene to Pd and to a lesser extent the more facile migratory insertion of carbonyl alkyl relative to ethylene alkyl complexes: $k_{\mathrm{e}}/k_{\mathrm{CO}} = 1/2000$.

Summary

A unique series of Pd(II) complexes have been developed which allow the first direct observation of three related classes of migratory insertion reactions with the same metal center. These include alkyl migrations to CO and to ethylene as well as acyl migrations to ethylene (Table 4). The $\Delta G^{\ddagger}$ for these reactions increase in the order $\Delta G^{\ddagger}_{\mathrm{R}\rightarrow\mathrm{CO}} \approx 15$ kcal/mol (−66 °C) < $\Delta G^{\ddagger}_{\mathrm{Ac}\rightarrow\mathrm{C_2H_4}} \approx 17$ kcal/mol (*ca.* −45 °C) < $\Delta G^{\ddagger}_{\mathrm{R}\rightarrow\mathrm{C_2H_4}} \approx 19$ kcal/mol (−25 °C). The rate of migratory insertion of the carbonyl alkyl complexes is not greatly affected by a change

(55) Turnover frequencies were measured as a function of gas uptake (1 atm of 1:1 ethylene/CO) at room temperature in a solvent mixture of CH_2Cl_2 and pentafluorophenol (10%), whose function is to solubilize the E/CO copolymer. Turnover frequencies of the related styrene/CO copolymer are unaffected by the presence of pentafluorophenol. Wagner, M. I.; Brookhart, M. Personal communication.

(56) Solutions of ethylene and **14** yield butenes and *intact* **14** at 20 °C; presumably, the migratory insertion product of **15** or an olefin hydride isomer of **14** reacts with ethylene to form trace amounts of **7** which dimerizes ethylene much faster than **7** is initially formed.

from CH_2Cl_2 ($\Delta G^{\ddagger} = 15.4 \pm 0.1$ kcal/mol) to the much more coordinating acetone-d_6 ($\Delta G^{\ddagger} = 15.15 \pm 0.1$ kcal/mol) or the presence of a tethered keto group on the growing polymer chain ($\Delta G^{\ddagger} = 15.0 \pm 0.1$ kcal/mol). The barriers to the alkyl and acyl migrations to ethylene increase slightly with increased substitution of the alkyl or acyl group. The difference in barriers for ethyl and methyl migration to ethylene is *ca.* 1 kcal/mol and the difference between $-C(O)CH_2CH_2C(O)CH_3$ and acetyl is *ca.* 0.5 kcal/mol.

The relative ground state stabilities of palladium ethylene, carbonyl, and 5- and 6-membered β- and γ-keto chelate species have been determined through a combination of competitive and relative equilibria studies. In all cases studied, CO binds the strongest to palladium. The binding affinities of L in (phen)-$Pd(CH_3)(L)^+$ decrease in the order CO > MeSPh > $CH_3CN \approx C_2H_4 > C_6H_5CN \gg OEt_2$. Also, the binding affinity of ethylene relative to CO increased for the series (phen)$Pd(R)(L)^+$ as a function of R: $CH_2CH_2C(O)CH_3$ ($K_6/K_1 = 0.33$) < CH_3 ($K_1/K_1 = 1$) < $C(O)CH_2CH_2C(O)CH_3$ ($K_5/K_1 = 7.2$) < $C(O)CH_3$ ($K_2/K_1 \approx 34$).

A mechanistic model for the copolymerization has been developed by combining the competitive binding studies and kinetic data of the migratory insertion reactions for (phen)Pd-$(C(O)CH_2CH_2C(O)CH_3)(L)^+$ and (phen)$Pd(CH_2CH_2C(O)CH_3)$-$(L)^+$ (L = C_2H_4, CO). The resting state is the carbonyl acyl species **18-P** (Scheme 9). Within the catalytic cycle, **18-P** must overcome a large equilibrium ($K_5(25°C) = (7.1 \pm 3.5) \times 10^{-4}$) to form the ethylene acyl complex, **17-P**, which undergos β-acyl migration in the turnover-limiting step. Subsequent formation of the carbonyl alkyl complex, **16-P**, followed by migratory insertion and CO trapping rapidly reform the resting state **18-P**. The 5- and 6-membered keto−chelate complexes **14-P** and **19-P** are at small concentrations during the copolymerization because of their large instability relative to their carbon monoxide coordinated open forms **16-P** and **18-P**, respectively. The kinetics of the combined microscopic steps of the propagation model (calculated TO frequency = $(16 \pm 12) \times 10^{-3}$ s^{-1}) closely match the experimental turnover frequency (8×10^{-3} s^{-1}) at 25 °C for the ethylene/CO copolymerization. The close agreement is surprising but may arise in part due to the inherently small contributions of $\Delta S°$ and $\Delta S^{\ddagger}$ to the preequilibrium between CO and ethylene binding and the intramolecular migratory insertion reaction of the ethylene acyl **17-P**, respectively.

Consecutive ethylene insertions are inhibited in two ways. First there is only a very small equilibrium concentration of the ethylene alkyl species, relative to the carbonyl alkyl complex, present ($K_6 = (9.9 \pm 5) \times 10^{-5}$). In addition, the rate of migratory insertion of carbonyl alkyl complexes is ca. 2000 times faster than their ethylene analogues. These combined results predict that consecutive ethylene insertions will occur roughly $1/10^6$ times and thus explain why the perfectly alternating structure of the ethylene/CO copolymer is obtained in this system.

Experimental Section

General Methods. All reactions, except where indicated, were carried out in flame-dried glassware under a dry, oxygen-free argon atmosphere using standard Schlenk and drybox techniques. Non-deuterated solvents were distilled under a nitrogen atmosphere from a drying agent immediatelty prior to use: CH_2Cl_2 from P_4O_{10}; hexanes and diethyl ether from sodium benzophenone ketyl. CD_2Cl_2 and $CDCl_2F$ were dried over CaH_2, submitted to 5 freeze−pump−thaw cycles and then vacuum transferred into glass Schlenk tubes fitted with Kontes high-vacuum Teflon plugs, and then stored under Ar. CP grade CO and ethylene were purchased from National Welders Supply and Matheson, respectively; both were used as received. When necessary, ethylene gas was added to the NMR sample, except where indicated otherwise, by slowly expelling a known volume of ethylene (1 atm at 22 °C) from a gas-tight syringe fitted with a 12 in. 22-gauge needle into the bottom of the CD_2Cl_2 solution at −78 °C without an outlet needle present. The volume of gas was taken as a rough guide to the number of equivalents of gas added while the actual number of ethylene equivalents in solution was determined by integration relative to the organometallic analyte.

The concentration of CO in a saturated CD_2Cl_2 solution was determined using Bryndza's empirical equation[50] determined from −80 to +20 °C:

$$[CO]_{sat} = (2.75 \times 10^{-6})T(°C) + (6.45 \times 10^{-3})$$

The increasing solubility of CO with temperature has been noted by others. For a brief discussion, see Fogg and Gerrard's text.[57]

NMR probe temperatures were measured using an anhydrous methanol sample except for temperatures below −95 °C, which were determined using a thermocouple. ^1H and ^{13}C chemical shifts were referenced to residual ^1H signals and to the ^{13}C signals of the deuterated solvents, respectively.

Atom-labeling schemes for the phenanthroline, bipyridine and $(3,5\text{-}(CF_3)_2C_6H_3)_4B^-$ counterion resonances are as follows:

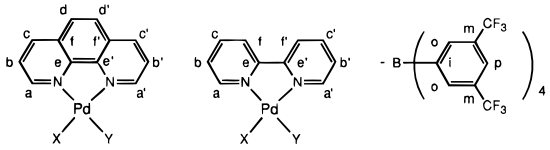

The ^1H NMR resonances were assigned into groups of a, b, c, d, f or a′, b′, c′, d′, f′ according to their characteristic coupling patterns. The ^{13}C NMR resonances were assigned in pairs such as C_a or $C_{a'}$ and $C_{a'}$ or C_a, based on their chemical shifts and $^1J_{CH}$. The relation betweeen the ^1H and ^{13}C assignments and the stereochemistry with respect to the ligands X,Y has not been ascertained.

Complexes **7**, **8**, and **13** undergo apparent *cis* ⇌ *trans* equilibration, exchanging the two chemically inequivalent sides of the phenanthroline ligand.[36,58−61] Therefore, NMR data are given for high- and low-temperature extremes.

Errors reported for rate constants determined are standard deviations of several experiments. Errors in $\Delta G^{\ddagger}$, $\Delta H^{\ddagger}$, and $\Delta S^{\ddagger}$ were calculated from the derivations of Binsch and Girolami respectively and incorporated a ±1° error in temperature.[62,63] Errors for rate constants and $\Delta G^{\ddagger}$ determined from DNMR spectroscopy incorporated a 20% error in rate and a ±1° error in temperature except when coalescence data were used, then a ± 5° error in temperature was used. Errors in $\Delta H°$ and $\Delta S°$ were calculated from the standard deviations of the slope and intercept of the van't Hoff plots. Calculation of σK_3 and σK_4 at 298 K included the covariance between $\Delta H°$ and $\Delta S°$ in analogy to Clifford's treatment of the Arrhenius equation.[64]

C, H, N analyses were performed by Oneida Research Laboratories of Whitesboro, NY.

$H^+(OEt_2)_2Ar'_4B^-$ [65] and $CDCl_2F$[66] (prepared by Dr. Brian Grant) were prepared according to literature procedures. The preparations of compounds (phen)$Pd(CH_3)(L)^+Ar'_4B^-$ (L = OEt_2 (**1**),[38] $NCCH_3$ (**5**)[67]

(57) Fogg, P. G. T.; Gerrard, W. *Solubility of Gases in Liquids: A Critical Evaluation of Gas/Liquid Systems in Theory and Practice*; John Wiley & Sons: New York, 1991.

(58) Cross, R. J. *Chem Soc. Rev.* **1985**, *14*, 197.

(59) Cooper, M. K.; Downes, J. M. *J. Chem. Soc., Chem. Commun.* **1981**, 381.

(60) Ozawa, F.; Ito, T.; Nakamura, Y.; Yamamoto, A. *Bull. Chem. Soc. Jpn.* **1981**, *54*, 1868.

(61) Komiya, S.; Albright, T. A.; Hoffmann, R.; Kochi, J. K. *J. Am. Chem. Soc.* **1976**, *98*, 7255.

(62) Binsch, G. In *Dynamic Nuclear Magnetic Resonance Spectroscopy*; Jackman, L., Cotton, F. A., Eds.; Academic Press: New York, 1975; p 77.

(63) Morse, P. M.; Spencer, M. D.; Wilson, S. R.; Girolami, G. S. *Organometallics* **1994**, *13*, 1646.

(64) Clifford, A. A. *Multivariate Error Analysis*; John Wiley and Sons: New York, 1973; pp 48−53.

(65) Brookhart, M.; Grant, B.; Volpe, A. F. *Organometallics* **1992**, *11*, 3920.

(66) Siegel, J. S.; Anet, F. A. *J. Org. Chem.* **1988**, *53*, 2629.

(67) Barborak, J. C.; Brookhart, M. S.; Rix, F. C.; Wagner, M. I. Manuscript in preparation.

(prepared by Mr. Mark Wagner)) and (phen)Pd$(CH_3)_2$[38,68] are reported elsewhere.

I. Preparations. (phen)Pd(Me)(CO)$^+$Ar′$_4$B$^-$ (2). A slurry of **1** was prepared *in situ* from (phen)Pd$(CH_3)_2$ (148 mg, 4.67×10^{-4} mol), $H^+(OEt_2)_2$Ar′$_4$B$^-$ (505 mg, 4.99×10^{-4} mol), and CH_2Cl_2 (1.5 mL) at −30 °C, and then diluted with additional CH_2Cl_2 (2.5 mL). Care was taken to wash down any (phen)Pd$(CH_3)_2$ from the sides of the flask since it decomposes to Pd black in the presence of CO. The mixture was warmed to dissolve the precipitate and then cooled to −78 °C. The solution was vigorously purged with CO for 1−5 min. After an additional 30 min at −78 °C, hexane (50 mL) was added to completely precipitate a white to off-white solid. The dried solid was dissolved in CH_2Cl_2 (1.5 mL), then cooled to −30 °C; hexane (0.2−0.5 mL) was added, yielding colorless crystals over time. After removing the mother liquor, the crystals were washed with hexane (2 × 5 mL) and dried *in vacuo*. **2** was obtained as a white solid (440 mg, 79%). Anal. Calcd for $C_{46}H_{23}BF_{24}N_2OPd$: C, 46.32; H, 1.94; N, 2.35. Found: C, 46.47; H, 2.00; N, 2.21.

IR (CH_2Cl_2) $\nu_{CO} = 2130$ cm^{-1}.

^{1}H NMR (300 MHz, CD_2Cl_2, 20 °C) δ 8.97 (dd, $J = 5.1$ Hz, $J = 1.5$ Hz, 2H, H_a and $H_{a'}$), 8.74 (dd, $J = 8.4$ Hz, $J = 1.5$ Hz, 1H, H_c or $H_{c'}$), 8.69 (dd, $J = 8.4$ Hz, $J = 1.5$ Hz, 1H, $H_{c'}$ or H_c), 8.10 (s, 2H, H_d and $H_{d'}$), 8.06 (dd, $J = 8.4$ Hz, $J = 5.4$ Hz, 1H, H_b or $H_{b'}$), 7.99 (dd, $J = 8.4$ Hz, $J = 5.1$ Hz, 2H, $H_{b'}$ or H_b), 7.72 (s, 8H, Ar′-H_o), 7.54 (s, 4H, Ar′-H_p), 1.66 (s, 3H, CH_3).

^{13}C NMR (75 MHz, CD_2Cl_2, 20 °C) δ 176.3 (s, CO), 162.19 (q, $^1J_{CB} = 50$ Hz, Ar′-C_i), 151.9 (d, $J_{CH} = 184$ Hz, C_a or $C_{a'}$), 148.1 (d, $J_{CH} = 184$ Hz, $C_{a'}$ or C_a), 148.0 (s, C_e or $C_{e'}$), 144.51 (s, $C_{e'}$ or C_e), 142.1 (d, $J_{CH} = 169$ Hz, C_c or $C_{c'}$), 140.8 (d, $J_{CH} = 168$ Hz, $C_{c'}$ or C_c), 135.2 (d, $J_{CH} = 161$ Hz, Ar′-C_o), 131.5 (s, C_f or $C_{f'}$), 131.1 (s, $C_{f'}$ or C_f), 129.3 (q, $^2J_{CF} = 31$ Hz, Ar′-C_m), 128.6 (d, $J_{CH} = 167$ Hz, C_d or $C_{d'}$), 128.3 (d, $J_{CH} = 172$ Hz, $C_{d'}$ or C_d), 127.0 (d, $J_{CH} = 171$ Hz, C_b or $C_{b'}$), 126.0 (d, $J_{CH} = 172$ Hz, $C_{b'}$ or C_b), 123.9 (q, $^1J_{CF} = 273$ Hz, Ar′-CF_3), 117.9 (d, $J_{CH} = 164$ Hz, Ar′-C_p), 5.39 (q, $J_{CH} = 141$ Hz, CH_3).

(phen)Pd(CH_3)(^{13}CO)$^+$Ar′$_4$B$^-$ (2*). Complex **2*** was prepared similarly from **1** and ^{13}CO. Spectral characteristics were identical to **2** except for:

IR (CH_2Cl_2) $\nu_{^{13}CO} = 2081$ cm^{-1}.

^{13}C(H) NMR (100 MHz, CD_2Cl_2, −80 °C) δ 5.8, (d, $^2J_{CC} = 3$ Hz, CH_3).

(phen)Pd$(CH_3)(C_2H_4)^+$Ar′$_4$B$^-$ (3). CD_2Cl_2 (0.35 mL) was added to a 5 mm NMR tube charged with **1** (12 mg, 9.6×10^{-6} mol) at −78 °C. The sample was warmed briefly to dissolve **1**, then approximately an equal volume of $CDCl_2F$ was cannulated onto this solution at −78 °C. To the mixed solution was added C_2H_4 (0.19 mL, ∼0.8 equiv). The ^{1}H NMR showed a small amount of unreacted **1**. A static spectrum was obtained at −110 °C; the two bound olefin resonances each exhibited a 6-line pattern consistent with an AA'BB' spin system. The second order coupling constants were not determined by simulation; however, $|\Delta\nu_{AB}| = 72.9$ Hz was determined.[69] The two multiplets coalesced at −81 °C, $k_{ex} = (162 \pm 32)$ s^{-1}, $\Delta G^{\ddagger} = 9.2 \pm 0.2$ kcal/mol. This experiment was repeated using 1.5 equiv of ethylene; one singlet was observed at δ 5.13 for both the coordinated and free ethylene resonances in the −110 °C ^{1}H NMR.

^{1}H NMR (400 MHz, −110 °C, ∼1CD_2Cl_2:∼1$CDCl_2F$) δ 8.82 (d, $J_{ab} = 5.20$ Hz, 1H, H_a), 8.54 (d, $J = 8.40$ Hz, 1H, H_c or $H_{c'}$), 8.41 (d, $J = 8.40$ Hz, 1H, $H_{c'}$ or H_c), 8.33 (d, $J_{a'b'} = 4.80$ Hz, 1H, $H_{a'}$), 7.92 (dd, $J_{b'c'} = 8.40$ Hz, $J_{a'b'} = 4.80$ Hz, 1H, $H_{b'}$), 7.90 (d, $J_{dd'} = 8.80$ Hz, 1H, H_d or $H_{d'}$), 7.87 (d, $J_{dd'} = 8.80$ Hz, 1H, $H_{d'}$ or H_d), 7.8 (m, 9H, Ar′-H_o + H_b), 7.49 (s, 4H, Ar′-H_p), 5.11 (m, 2H, $H_AH_BC{=}CH_{A'}H_{B'}$), 4.93 (m, 2H, $H_AH_BC{=}CH_{A'}H_{B'}$), 0.920 (s, 3H, CH_3).

^{13}C NMR (75 MHz, −85 °C, CD_2Cl_2) δ 161.2 (q, $^1J_{CB} = 49$ Hz, Ar′-C_i), 146.9 (d, $J_{CH} = 186$ Hz, C_a or $C_{a'}$), 146.0 (d, $J_{CH} = 182$ Hz, $C_{a'}$ or C_a), 145.9 (s, C_e or $C_{e'}$), 143.6 (s, $C_{e'}$ or C_e), 140.6 (d, $J_{CH} = 166$ Hz, C_c or $C_{c'}$), 133.9 (d, $J_{CH} = 169$ Hz, $C_{c'}$ or C_c), 135.0 (d, $J_{CH} = 159$ Hz, Ar′-C_o), 129.8 (s, C_f or $C_{f'}$), 129.7 (s, $C_{f'}$ or C_f), 127.9 (q, $^2J_{CF} = 28$ Hz, Ar′-C_m), 127.2 (d, $J_{CH} = 167$ Hz, C_d or $C_{d'}$), 127.0 (d, $J_{CH} = 166$ Hz, $C_{d'}$ or C_d), 125.4 (d, $J_{CH} = 171$ Hz, C_b or $C_{b'}$), 124.8 (d, $J_{CH} = 170$ Hz, $C_{b'}$ or C_b), 123.7 (q, $^1J_{CF} = 272$ Hz, Ar′-CF_3), 116.9 (d, $J_{CH} = 164$ Hz, Ar′-C_p), 86.4 (t, $J_{CH} = 163$ Hz, C_2H_4), 11.2 (q, $J_{CH} = 138$ Hz, CH_3).

(phen)Pd(CH_3)(S$(CH_3)(C_6H_5)$)$^+$Ar′$_4$B$^-$ (4). Thioanisole (19 μL, 1.6×10^{-4} mol) was added to a cooled (−30 °C) solution of CH_2Cl_2 (2 mL) and **1** (200 mg, 1.6×10^{-4} mol). After 30 min, hexane (0.1 mL) was added and the solution slowly cooled to −78 °C. Yellow crystals formed. At −78 °C, the mother liquor was removed; the crystals were washed with CH_2Cl_2 (2 × 0.5 mL) and hexanes (2 × 5 mL) and then dried *in vacuo* at 20 °C to give **4** (167 mg, 81%) as a yellow solid. Anal. Calcd for $C_{52}H_{31}N_2B_1S_1F_{24}Pd_1$: C, 48.45; H, 2.42; N, 2.17. Found: C, 48.82; H, 2.25; N, 1.82.

^{1}H NMR (300 MHz, CD_2Cl_2, −66 °C) δ 9.01 (dd, $J = 5.1$ Hz, $J = 1.3$ Hz, 1H, H_a or $H_{a'}$), 8.91 (dd, $J = 5.4$ Hz, $J = 1.3$ Hz, 1H, $H_{a'}$ or H_a), 8.63 (dd, $J = 8.1$ Hz, $J = 1.3$ Hz, 1H, H_c or $H_{c'}$), 8.58 (dd, $J = 8.3$ Hz, $J = 1.3$ Hz, 1H, $H_{c'}$ or H_c), 8.02 (s, 2H, H_d + $H_{d'}$), 7.93 (m, 2H, H_b +$H_{b'}$), 7.72 (m, 10H, Ar′-H_o (8H) + SPh (2H)), 7.51 (s, 4H, Ar′-H_p), 7.43 (m, 3H, SPh), 2.88 (s, 3H, SCH_3), 1.04 (s, 3H, $PdCH_3$).

^{13}C NMR (75 MHz, CD_2Cl_2, 20°) δ 162.19 (q, $^1J_{CB} = 50$ Hz, Ar′-C_i), 148.9 (d, $J_{CH} = 185$ Hz, C_a or $C_{a'}$), 148.4 (d, $J_{CH} = 183$ Hz, $C_{a'}$ or C_a), 147.7 (s, C_e or $C_{e'}$), 145.3 (s, $C_{e'}$ or C_e), 140.6 (d, $J_{CH} = 167$ Hz, C_c or $C_{c'}$), 139.7 (d, $J_{CH} = 167$ Hz, $C_{c'}$ or C_c), 135.3 (d, $J_{CH} = 161$ Hz, Ar′-C_o), 131.3 (s, C_f or $C_{f'}$), 131.1 (s, SPh-C_i), 131.0 (s, $C_{f'}$ or C_f), 130.5 (d, $J_{CH} = ca.$ 170 Hz, SPh-C_p), 130.4 (d, $J_{CH} = ca.$ 175 Hz, SPh-C_o or SPh-C_m), 130.3 (d, $J_{CH} = ca.$ 175 Hz, SPh-C_m or SPh-C_o), 129.3 (q, $^2J_{CF} = 31$ Hz, Ar′-C_m), 128.3 (d, $J_{CH} = 167$ Hz, C_d or $C_{d'}$), 128.0 (d, $J_{CH} = 166$ Hz, $C_{d'}$ or C_d), 126.2 (d, $J_{CH} = 170$ Hz, C_b or $C_{b'}$), 125.8 (d, $J_{CH} = 171$ Hz, $C_{b'}$ or C_b), 123.9 (q, $^1J_{CF} = 273$ Hz, Ar′-CF_3), 118.0 (d, $J_{CH} = 164$ Hz, Ar′-C_p), 22.1, (q, $J_{CH} = 144$ Hz, SCH_3), 10.0 (q, $J_{CH} = 135$ Hz, $PdCH_3$).

(phen)Pd(CH_3)(NC$_6H_5)^+$Ar′$_4$B$^-$ (6). CH_2Cl_2 (2 mL) was added to (phen)Pd$(CH_3)_2$ (148 mg, 4.67×10^{-4} mol) and $H^+(OEt_2)_2$Ar′$_4$B$^-$ (525 mg, 5.19×10^{-4} mol) at −30 °C. After 20 min, benzonitrile (53 μL, 5.2×10^{-4} mol) was added. Following an additional 30 min at −30 °C, the yellow solution was warmed to 20 °C and stirred for 15 min. Cooling to −78 °C over a 10 h period, with the slow additon of hexanes (0.7 mL overall), gave a light yellow crystalline product. At −78 °C, the mother liquor was removed and the product washed with CH_2Cl_2 (2 × 0.5 mL), and then hexanes (5 mL). The product was warmed to 20 °C, washed with additional hexanes, (5 mL) and dried *in vacuo*, yield 581 mg (98%). Anal. Calcd for $C_{52}H_{28}BF_{24}N_3Pd$: C, 49.26; H, 2.23; N, 3.31. Found: C, 49.28 ; H, 2.15; N, 3.31.

^{1}H NMR (400 MHz, CD_2Cl_2, 20 °C) δ 8.95 (dd, $J_{ab} = 5.5$ Hz, $J_{ac} = 1.4$ Hz, 1H, H_a), 8.92 (dd, $J_{a'b'} = 5.0$ Hz, $J_{a'c'} = 1.5$ Hz, 1H, $H_{a'}$), 8.63 (dd, $J_{bc} = 8.3$ Hz, $J_{ac} = 1.4$ Hz, 1H, H_c), 8.59 (dd, $J_{b'c'} = 8.4$ Hz, $J_{a'c'} = 1.5$ Hz, 1H, $H_{b'}$), 8.04 (d, $J_{d,d'} = 11.0$ Hz, 1H, H_d), 8.03 (d, $J_{d,d'} = 11.0$ Hz, 1H, $H_{d'}$), 7.96−7.9 (m, 4H, $H_{b,b'}$ (2H) + Ph (2H)), 7.83 (t, $J = 8$ Hz, 1H, Ph-H_p), 7.77 (m, 8H, Ar′-H_o), 7.64 (t, $J = 8$ Hz, 2H, Ph), 7.57 (s, 4H, Ar′-H_p), 1.41 (s, 3H, CH_3).

^{13}C NMR (100 MHz, CD_2Cl_2, 20 °C) δ 162.2 (q, $^1J_{CB} = 50$ Hz, C_i), 149.7 (d, $J_{CH} = 187$ Hz, C_a or $C_{a'}$), 148.9 (d, $J_{CH} = 184$ Hz, $C_{a'}$ or C_a), 148.4 (s, C_e or $C_{e'}$), 144.5 (s, $C_{e'}$ or C_e), 140.3 (d, $J_{CH} = 167$ Hz, C_c or $C_{c'}$), 139.5 (d, $J_{CH} = 166$ Hz, $C_{c'}$ or C_c), 136.0 (d, $J_{CH} = 166$ Hz, Ph-C_p), 135.2 (d, $J_{CH} = 160$ Hz, Ar′-C_o), 133.5 (d, $J_{CH} \sim 175$ Hz half of doublet is obscured by Ar′-C_o, Ph-C), 131.2 (s, C_f or $C_{f'}$), 130.6 (s, $C_{f'}$ or C_f), 130.3 (d, $J_{CH} = 160$ Hz, Ph-C), 129.4 (q, $^2J_{CF} = 33$ Hz, Ar′-C_m), 128.2 (d, $J_{CH} = 167$ Hz, C_d or $C_{d'}$), 127.9 (d, $J_{CH} = 167$ Hz, $C_{d'}$ or C_d), 126.3 (d, $J_{CH} = 170$ Hz, C_b or $C_{b'}$), 125.0 (q, $^1J_{CF} = 273$ Hz, Ar′-CF_3), 125.8 (d, $J_{CH} = 172$ Hz, $C_{b'}$ or C_b), 123.4 (s, N*C*Ph), 117.9 (d, $J_{CH} = 164$ Hz, Ar′-C_p), 109.4 (s, Ph-C_i), 3.9 (q, $J_{CH} = 136$ Hz, CH_3).

(phen)Pd$(CH_2CH_3)(C_2H_4)^+$Ar′$_4$B$^-$ (7). CD_2Cl_2 (0.7 mL) was added to a 5 mm NMR tube charged with **1** (30 mg, 24×10^{-6} mol) at −78 °C and warmed briefly to dissolve the solid. An ethylene purge through the solution was begun at −78 °C and then continued as the temperature was raised to +5 °C (ice bath) where the purge was continued for 30 min. After this time, approximately 0.2 mL of a clear yellow solution remained. After cooling to −78 °C, propane (∼1 mL) was condensed into the NMR tube precipitating an off-white solid. The propane and CD_2Cl_2 were cannulated off of the solid. After washing with propane (2 × ∼1 mL), the sample was dried under vacuum, via a needle inserted through the septum into the NMR tube. CD_2Cl_2 (0.7 mL) was slowly

(68) Byers, P. K.; Canty, A. J. *Organometallics* **1990**, *9*, 210.

(69) Hoffman, R. A.; Forsén, S.; Gestblom, B. In *NMR Basic Principles and Progress*; Diehl, P., Fluck, E., Kosfeld, R., Eds.; Springer Verlag: New York, 1971; Vol. 5, p 118.

dripped down the cold sides of the tube at −78 °C. After agitating briefly to dissolve the solid, taking care to keep the NMR tube cold, the sample was placed in a precooled NMR probe (−85 °C) and the ^{13}C NMR obtained. Afterwards, ca. half the solution was removed via cannula and about an equal volume of $CDCl_2F$ was added to the tube. The sample was placed in a precooled NMR probe (−80 °C); ^{1}H NMR were subsequently recorded at various temperatures. A static spectrum was obtained at −110 °C; the two bound olefin resonances exhibited a broad AB pattern, $\Delta\nu = 138$ Hz. The two multiplets coalesced at −75.6 °C, $k_{ex} = 306 \pm 61$ s^{-1}, $\Delta G^{\ddagger} = 9.2 \pm 0.2$ kcal/mol. The C**H**$_2$-CH$_3$ and CH$_2$C**H**$_3$ resonances were broadened in the −110 °C ^{1}H NMR spectrum.

^{1}H NMR (400 MHz, −110 °C, ∼1CD_2Cl_2:∼1$CDCl_2F$) δ 8.90 (d, $J_{ab} = 5.20$ Hz, 1H, H$_a$), 8.57 (d, $J = 8$ Hz, 1H, H$_c$ or H$_{c'}$), 8.43 (d, $J = 8$ Hz, 1H, H$_{c'}$ or H$_c$), 8.34 (d, $J_{a'b'} = 5$ Hz, 1H, H$_{a'}$), 8.02 (dd, $J_{bc} = 8$ Hz, $J_{ab} = 5.2$ Hz, 1H, H$_b$), 7.91 (m, 2H, H$_d$ and H$_{d'}$), 7.78 (m, 9H, Ar′-H$_o$ + H$_b$), 7.49 (s, 4H, Ar′-H$_p$), 5.14 (m, 2H, $H_AH_BC{=}CH_{A'}H_{B'}$), 4.79 (m, 2H, $H_AH_BC{=}CH_{A'}H_{B'}$), 1.69 (broad q, $J \sim 8$ Hz, 2H, CH$_2$), 1.04 (broad t, $J \sim 8$ Hz, 2H, CH$_2$).

^{13}C NMR (75 MHz, CD_2Cl_2, −85 °C) δ 161.8 (q, $^1J_{CB} = 50$ Hz, Ar′-C$_i$), 147.1 (d, $J_{CH} = 185$ Hz, C$_a$ or C$_{a'}$), 146.4 (d, $J_{CH} = 181$ Hz, C$_{a'}$ or C$_a$), 145.7 (s, C$_e$ or C$_{e'}$), 143.1 (s, C$_{e'}$ or C$_e$), 140.8 (d, $J_{CH} = 168$ Hz, C$_c$ or C$_{c'}$), 139.3 (d, $J_{CH} = 168$ Hz, C$_{c'}$ or C$_c$), 134.0 (d, $J_{CH} = 160$ Hz, Ar′-C$_o$), 129.9 (s, C$_f$ or C$_{f'}$), 129.6 (s, C$_{f'}$ or C$_f$), 128.4 (q, $^2J_{CF} = 32$ Hz, Ar′-C$_m$), 127.5 (d, $J_{CH} = 167$ Hz, C$_d$ or C$_{d'}$), 127.2 (d, $J_{CH} = 167$ Hz, C$_{d'}$ or C$_d$), 125.5 (d, $J_{CH} = 170$ Hz, C$_b$ or C$_{b'}$), 125.4 (d, $J_{CH} = 171$ Hz, C$_{b'}$ or C$_b$), 123.8 (q, $^1J_{CF} = 272$ Hz, Ar′-CF$_3$), 117 (d, $J_{CH} = 165$ Hz, Ar′-C$_p$), 87.0 (t, $J_{CH} = 161$ Hz, C_2H_4), 28.3 (t, $J_{CH} = 138$ Hz, CH$_2$), 16.0 (multiplet was obscured by propane resonance, CH$_3$).

^{1}H NMR of **3** during ethylene dimerization at low percent conversion.

^{1}H NMR (300 MHz, CD_2Cl_2, −24.7 °C) δ 8.85 (br s, 1H, H$_a$ or H$_{a'}$), 8.65 (s, br, 2H, H$_c$ or H$_{c'}$), 8.41 (s, br, 1H, H$_{a'}$ or H$_a$), 8.06 (s, 2H, H$_d$ or H$_{d'}$), 8.0 (s, br, 2H, H$_c$ or H$_{c'}$), 7.72 (m, 8H, Ar′-H$_o$), 7.53 (s, 4H, Ar′-H$_p$), 1.82 (q, $J = 7.61$ Hz, 2H, PdCH_2CH$_3$), 1.10 (t, $J = 7.61$ Hz, 3H, PdCH$_2$CH_3). Free and coordinated ethylene resonances are time averaged.

(phen)Pd(C(O)Me)(CO)$^+$Ar′$_4$B$^-$·CH$_2$Cl$_2$ (8·CH$_2$Cl$_2$). Complex **2** (500 mg, 4.2×10^{-4} mol) in CH_2Cl_2 (3.5 mL) was purged with CO for 1 min at 20 °C. A small amount of a fine black powder formed. The mixture was filtered through Celite (1 cm) and the Celite was washed with CH_2Cl_2 (10 mL). The filtrate was reduced to a glass *in vacuo*. CH_2Cl_2 (4 mL) was added to the glass. The yellow solution was purged with CO for 1 min. Under a CO atmosphere, hexane (2 mL) was added; slow cooling to −20 °C (1 h) and then to −78 °C gave **8**·CH_2Cl_2 as light yellow crystals (455 mg, 88%). Anal. Calcd for $C_{48}H_{25}BCl_2F_{24}N_2O_2Pd$: C, 44.15; H, 1.93; N, 2.15. Found: C, 44.68; H, 1.85; N, 2.03.

IR (CH_2Cl_2) $\nu_{CO} = 2128$ (PdCO), 1748 (C(O)CH$_3$) cm^{-1}.

^{1}H NMR (300 MHz, CD_2Cl_2, 20 °C) δ 8.74 (d, $J_{ab} = 5.0$ Hz, 2H, H$_a$ and H$_{a'}$), 8.68 (d, $J_{ac} = 8.2$ Hz, 2H, H$_c$ and H$_{c'}$), 8.07 (s, 2H, H$_d$ and H$_{d'}$), 7.98 (dd, $J_{ac} = 8.2$ Hz, $J_{ab} = 5.0$ Hz, 2H, H$_b$ and H$_{b'}$), 7.73 (s, 8H, Ar′-H$_o$), 7.54 (s, 4H, Ar′-H$_p$), 2.93 (s, 3H, CH$_3$).

^{13}C NMR (75 MHz, CD_2Cl_2, 20 °C) δ 214.3 (s, *C*(O)CH$_3$), 174.1 (s, PdCO), 162.1 (q, $^1J_{CB} = 50$ Hz, Ar′-C$_i$), 151.7 (d, $J_{CH} = 185$ Hz, C$_a$ and C$_{a'}$), 141.5 (d, $J_{CH} = 167$ Hz, C$_c$ and C$_{c'}$), 135.2 (d, $J_{CH} = 159$ Hz, Ar′-C$_o$), 131.1 (s, C$_f$ and C$_{f'}$), 129.3 (q, $^2J_{CF} = 31$ Hz, Ar′-C$_m$), 128.5 (d, $J_{CH} = 164$ Hz, C$_d$ and C$_{d'}$), 126.7 (d, $J_{CH} = 171$ Hz, C$_b$ and C$_{b'}$), 125.0 (q, $^1J_{CF} = 269$ Hz, Ar′-CF$_3$), 117.9 (d, $J_{CH} = 164$ Hz, Ar′-C$_p$), 40.7 (q, $J_{CH} = 132$ Hz, CH$_3$). The ipso resonances C$_e$ and C$_{e'}$ are broadened due to exchange and thus are not visible (see below).

^{1}H NMR (300 MHz, CD_2Cl_2, −57.2 °C) δ 8.80 (dd, $J_{ab} = 4.83$ Hz, $J_{ac} = 1.38$ Hz, 1H, H$_a$), 8.67 (dd, $J_{bc} = J_{b'c'} = 8.28$ Hz, $J_{ac} = J_{a'c'} = 1.38$ Hz, 1H, H$_c$ or H$_{c'}$), 8.62 (dd, $J_{bc} = J_{b'c'} = 8.28$ Hz, $J_{ac} = J_{a'c'} = 1.38$ Hz, 1H, H$_{c'}$ or H$_c$), 8.58 (dd, $J_{a'b'} = 5.17$ Hz, $J_{a'c'} = 1.38$ Hz, 1H, H$_{a'}$), 8.05 (d, $J_{dd'} = 8.97$ Hz, 1H, H$_d$ or H$_{d'}$), 8.02 (d, $J_{dd'} = 8.97$ Hz, 1H, H$_{d'}$ or H$_d$), 7.97 (dd, $J_{b'c'} = 8.28$ Hz, $J_{a'b'} = 5.17$ Hz, 1H, H$_{b'}$), 7.93 (dd, $J_{bc} = 8.28$ Hz, $J_{ab} = 4.83$ Hz, 1H, H$_b$), 7.72 (s, 8H, Ar′-H$_o$), 7.52 (s, 4H, Ar′-H$_p$), 2.92 (s, 3H, CH$_3$).

^{13}C NMR (75 MHz, CD_2Cl_2, −57.2 °C) δ 216.5 (s, *C*(O)CH$_3$), 173.0 (s, PdCO), 161.6 (q, $^1J_{CB} = 50$ Hz, Ar′-C$_i$), 151.2 (d, $J_{CH} = 185$ Hz, C$_a$ or C$_{a'}$), 151.1 (d, $J_{CH} = 186$ Hz, C$_{a'}$ or C$_a$), 145.4 (s, C$_e$ or C$_{e'}$), 143.1 (s, C$_{e'}$ or C$_e$), 141.5 (d, $J_{CH} = 169$ Hz, C$_c$ or C$_{c'}$), 140.4 (d, $J_{CH} = 167$ Hz, C$_{c'}$ or C$_c$), 134.5 (d, $J_{CH} = 160$ Hz, Ar′-C$_o$), 130.3 (s, C$_f$ or C$_{f'}$), 130.2 (s, C$_{f'}$ or C$_f$), 128.5 (q, $^2J_{CF} = 32$ Hz, Ar′-C$_m$), 128.0 (d, $J_{CH} = 168$ Hz, C$_d$ or C$_{d'}$), 127.6 (d, $J_{CH} = 168$ Hz, C$_{d'}$ or C$_d$), 126.4 (d, $J_{CH} = 171$ Hz, C$_b$ or C$_{b'}$), 126.0 (d, $J_{CH} = 171$ Hz, C$_{b'}$ or C$_b$), 124.2 (q, $^1J_{CF} = 272$ Hz, Ar′-CF$_3$), 117.3 (d, $J_{CH} = 167$ Hz, Ar′-C$_p$), 40.9 (q, $J_{CH} = 132$ Hz, CH$_3$).

(phen)Pd(CH(CO$_2$CH$_3$)CH$_2$C(O)CH$_3$)$^+$Ar′$_4$B$^-$ (9). Methyl acrylate (8 μL, 8.8×10^{-5} mol) was syringed onto **2** (100 mg, 8.4×10^{-5} mol) and CH_2Cl_2 (1.5 mL) at 20 °C, giving a bright yellow solution. After stirring for 15 min, the solvent was removed to give a yellow oil. The oil was washed with hexane (20 mL) and dried *in vacuo* to give a light-yellow glass (90 mg, 84%). The ^{13}CO labeled isotopomer, **9***, was prepared similarly. Anal. Calcd for $C_{50}H_{29}F_{24}N_2O_3Pd$: C, 46.96; H, 2.29; N, 2.19. Found: C, 46.46; H, 2.21; N, 2.04.

^{1}H NMR (300 MHz, CD_2Cl_2, 20 °C) δ 9.21 (dd, $J_{ab} = 5.57$ Hz, $J_{ac} = 1.47$ Hz, 1H, H$_a$), 8.96 (dd, $J_{a'b'} = 4.93$ Hz, $J_{a'c'} = 1.40$ Hz, 1H, H$_{a'}$), 8.61 (dd, $J_{bc} = 8.36$ Hz, $J_{ac} = 1.47$ Hz, 1H, H$_c$), 8.61 (dd, $J_{b'c'} = 8.26$ Hz, $J_{a'c'} = 1.40$ Hz, 1H, H$_{c'}$), 8.04 (d, $J_{dd'} = 8.88$ Hz, 1H, H$_d$ or H$_{d'}$), 7.99 (d, $J_{dd'} = 8.88$ Hz, 1H, H$_{d'}$ or H$_d$), 7.93 (dd, $J_{b'c'} = 8.26$ Hz, $J_{a'b'} = 4.93$ Hz, 1H, H$_{b'}$), 7.81 (dd, $J_{bc} = 8.36$ Hz, $J_{ab} = 5.57$ Hz, 1H, H$_b$), 7.76 (s, 8H, Ar′ H$_o$), 7.57 (s, 4H, Ar′ H$_p$), 3.66 (s, 3H, CO$_2$CH$_3$), 3.49 (d, $J_{HH} = 6.6$ Hz, CH), 3.18 (dd, $^2J_{HH} = 19.2$ Hz, $^3J_{HH} = 6.6$ Hz, CH_AH_B), 2.89 (d, $^2J_{HH} = 19.2$ Hz, CH$_A$H$_B$), 2.65 (s, 3H, Pd-OCCH$_3$).

^{13}C NMR (75.4 MHz, CD_2Cl_2, 20 °C) δ 241.0 (s, Pd-O*C*), 177.4 (s, *C*O$_2$Me), 162.2 (q, $^1J_{CB} = 50.0$ Hz, Ar′ C$_i$), 154.1 (d, $J_{CH} = 188.3$ Hz, C$_a$ or C$_{a'}$),149.6 (d, $J_{CH} = 186.1$ Hz, C$_{a'}$ or C$_a$), 148.0 (s, C$_e$ or C$_{e'}$), 144.7 (s, C$_{e'}$ or C$_e$), 140.3 (d, $J_{CH} = 167.8$ Hz, C$_c$ or C$_{c'}$), 139.9 (d, $J_{CH} = 167.3$ Hz, C$_{c'}$ or C$_c$), 135.2 (d, $J_{CH} = 159.7$ Hz, Ar′ C$_o$), 131.0 (s, C$_f$ or C$_{f'}$), 130.6 (s, C$_{f'}$ or C$_f$), 129.3 (q, $^2J_{CF} = 31$ Hz, Ar′ C$_m$), 128.1 (d, $J_{CH} = 167.4$ Hz, C$_d$ or C$_{d'}$), 127.9 (d, $J_{CH} = 167.5$ Hz, C$_{d'}$ or C$_d$), 126.4 (d, $J_{CH} = 170.2$ Hz, C$_b$ or C$_{b'}$), 126.3 (d, $J_{CH} = 170.8$ Hz, C$_{b'}$ or C$_b$), 125 (q, $^1J_{CF} = 273$ Hz, Ar′ CF$_3$), 117.8 (d, $J_{CH} = 164.1$ Hz, Ar′ C$_4$), 52.3 (q, $J_{CH} = 147.1$ Hz, CO$_2$**C**H$_3$), 51.7 (dd, $J_{CHA} = 133.8$ Hz, $J_{CHB} = 123.7$ Hz, CH$_2$), 36.7 (d, $J_{CH} = 146.2$ Hz, CH), 28.6 (q, $J_{CH} = 130.0$ Hz, CH$_3$).

9*: ^{13}C NMR (100 MHz, CD_2Cl_2, 20 °C) δ 51.7 (d, $^1J_{CC} = 42.1$ Hz, CH$_2$), 36.7 (d, $^2J_{CC} = 1.8$ Hz, CH), 28.6 (d, $^1J_{CC} = 40.4$ Hz, CH$_3$).

2 + acetone-d$_6$ ⇌ (phen)Pd(C(O)Me)(acetone-*d*$_6$)$^+$Ar′$_4$B$^-$ (10). (a) Equilibrium Study. Acetone-d_6 (0.7 mL) was added to a 5-mm NMR tube charged with **2** (10 mg, 8.0×10^{-6} mol) at −78 °C. The sample was warmed briefly to dissolve **2** and returned to the −78 °C bath. The sample was placed in a precooled NMR probe and the ^{1}H NMR recorded. A temperature dependent equilibrium between **2** and **10** was observed:

T (K)	208.3	226.9	249.3	271.6
K_{eq}	0.234	0.11	0.051	0.023

A van't Hoff plot created from ln(K_{eq}) versus 1/T gave $\Delta H° = -4.1 \pm 0.2$ kcal/mol, $\Delta S° = -22 \pm 0.6$ eu.

10: ^{1}H NMR (300 MHz, acetone-d_6, −64.9 °C) δ 9.00 (dd, $J_{bc} = 8.20$ Hz, $J_{ac} = 1.35$ Hz, 1H, H$_c$), 8.91 (dd, $J_{b'c'} = 8.27$ Hz, $J_{a'c'} = 1.41$ Hz, 1H, H$_{c'}$), 8.83 (dd, $J_{ab} = 5.22$ Hz, $J_{ac} = 1.35$ Hz, 1H, H$_a$), 8.75 (dd, $J_{a'b'} = 4.81$ Hz, $J_{a'c'} = 1.41$ Hz, 1H, H$_{a'}$), 8.31 (s, 2H, H$_d$ and H$_{d'}$), 8.21 (dd, $J_{bc} = 8.20$ Hz, $J_{ab} = 5.22$ Hz, 1H, H$_b$), 8.09 (dd, $J_{b'c'} = 8.27$ Hz, $J_{a'b'} = 4.81$ Hz, 1H, H$_{b'}$), 7.83 (m, 8H, Ar′-H$_o$), 7.74 (s, 4H, Ar′-H$_p$), 2.57 (s, 3H, C(O)CH$_3$).

The carbonyl chemical shifts were obtained upon repeating this experiment with (phen)Pd(CH$_3$)(^{13}CO)$^+$.

^{13}C{^{1}H} NMR (75.4 MHz, CD_2Cl_2, −80 °C) δ 224.6 (**10** *C*(O)-CH$_3$), 175.6 (**2** CO).

Complexes **8** (δ 3.1) (6.5%) and (phen)Pd(CH$_3$)(acetone-d_6)$^+$ (4%) (**11**) were also observed. Compound **11** was independently prepared from (phen)Pd(CH$_3$)OEt$_2$)$^+$ (**2**) and acetone-d_6.

11: ^{1}H NMR (300 MHz, acetone-d_6, 20 °C) δ 9.08 (dd, $J_{ab} = 5.3$ Hz, $J_{ac} = 1.5$ Hz, 1H, H$_a$), 9.00 (dd, $J_{a'b'} = 8.5$ Hz, $J_{a'c'} = 1.5$ Hz, 1H, H$_{c'}$ or H$_c$), 8.93 (dd, $J_{bc} = 8.5$ Hz, $J_{ac} = 1.5$ Hz, 1H, H$_c$ or H$_{c'}$), 8.76 (dd, $J = 5$ Hz, $J = 1.5$ Hz, 1H, H$_{a'}$), 8.32 (s, 2H, H$_d$ and H$_{d'}$), 8.16 (dd, $J = 8.5$ Hz, $J = 5.3$ Hz, 1H, H$_b$), 8.10 (dd, $J = 8.5$ Hz, $J = 5$ Hz, 1H, H$_{b'}$), 7.78 (m, 8H, Ar′-H$_o$), 7.66 (s, 4H, Ar′-H$_p$), 1.09 (s, 3H, CH$_3$).

(b) Temperature Jump Kinetics Experiment. The sample was warmed to ca. 40 °C and then inserted into a precooled (208.3 K) NMR probe. After 5 min of temperature stabilization, the approach to equilibrium was monitored over a 3.5 h period. The slope of the plot of $-\ln[([\mathbf{10}]_t - [\mathbf{10}]_\infty)/([\mathbf{10}]_0 - [\mathbf{10}]_\infty)]$ versus time ([acetone-d_6] = 13.60 M) gave the sum (k_1/k_{-1}[acetone-d_6]). Substitution into K_{eq}[acetone-d_6] = (k_1/k_{-1}[acetone-d_6]) gave values of k_1 and (k_{-1}/[acetone-d_6]). Averaged results from two experiments are as follows: K_{eq} = 3.18 ± 0.3; $k_1 = (5.5 \pm 0.8) \times 10^{-4}$ s^{-1}, $\Delta G^{\ddagger}_1 = 15.15 \pm 0.1$ kcal/mol; $k_{-1} = (1.8 \pm 0.4) \times 10^{-4}$ s^{-1}, $\Delta G^{\ddagger}_{-1} = 15.6 \pm 0.1$ kcal/mol.

(bipy)Pd(CH$_3$)(CO)$^+$Ar′$_4$B$^-$ (12). Complex **12** was prepared in a similar manner to **2** from (bipy)Pd(CH$_3$)$_2$ (137 mg, 4.67×10^{-4} mol), H$^+$ (OEt$_2$)$_2$Ar′$_4$B$^-$ (505 mg, 0.499 mol), and CO. Anal Calcd for $C_{44}H_{23}BF_{24}N_2OPd$: C, 45.21; H, 1.98; N, 2.39. Found: C, 45.31; H, 2.03; N, 2.29.

IR (CH_2Cl_2) ν_{CO} = 2130 cm^{-1}.

^{1}H NMR (400 MHz, CD_2Cl_2, 20 °C) δ 8.62 (m, 2H, H$_{a,a'}$), 8.24 (m, 4H, H$_{f,f'}$ + H$_{c,c'}$), 7.78 (m, 2H, H$_{b,b'}$), 7.72 (s, 8H, Ar′-H$_o$), 7.55 (s, 4H, Ar′-H$_p$), 1.49 (s, 3H, CH$_3$).

^{13}C NMR (100 MHz, CD_2Cl_2, 20 °C) δ 176.0 (s, Pd-CO), 162.2 (q, J_{CB} = 50 Hz, Ar′-C$_i$), 157.4 (s, C$_e$ or C$_{e'}$), 153.3 (s, C$_{e'}$ or C$_e$), 151.9 (d, J_{CH} = 184 Hz, C$_a$ or C$_{a'}$), 147.8 (d, J_{CH} = 187 Hz, C$_{a'}$ or C$_a$), 142.9 (d, J_{CH} = 170 Hz, C$_c$ or C$_{c'}$), 142.0 (d, J_{CH} = 170 Hz, C$_{c'}$ or C$_c$), 135.2 (d, J_{CH} = 160 Hz, Ar′-C$_o$), 129.3 (q, $^2J_{CF}$ = 31 Hz, Ar′-C$_m$), 128.9 (d, J_{CH} = 181 Hz, C$_f$ or C$_{f'}$), 128.1 (d, J_{CH} = 180 Hz, C$_{f'}$ or C$_f$), 125.0 (q, $^1J_{CF}$ = 273 Hz, Ar′-*C*F$_3$), 124.1 (d, J_{CH} = 168 Hz, C$_b$ or C$_{b'}$), 123.8 (d, J_{CH} = 168 Hz, C$_{b'}$ or C$_b$), 117.8 (d, J_{CH} = 164 Hz, Ar′-C$_p$), 5.8 (q, J_{CH} = 140 Hz, CH$_3$).

(phen)Pd(C(O)CH$_3$)(C$_2$H$_4$)$^+$Ar′$_4$B$^-$ (13). A ^{13}C NMR sample was prepared as follows: CD_2Cl_2 (0.7 mL) was vacuum transferred from CaH_2 onto **2** (30 mg, 2.5×10^{-5} mol) in a 5-mm J. Young NMR tube at liquid nitrogen temperature. The sample was warmed briefly to dissolve **2**. Ethylene (15 mL of gas) was vacuum transferred into the NMR tube with **2** at liquid nitrogen temperature. The sample was warmed to −78 °C and the tube agitated while cold to partially dissolve the precipitate. The sample was placed in a precooled (−66 °C) NMR probe and the formation of **13** and minor amounts of **3**, **14**, **15**, and **17** observed as described below in Section II(c). After 4 h the sample was removed from the probe; it was observed to be homogeneous and then placed under vacuum (0.01 mmHg) at −78 °C overnight, removing ∼$^1/_3$ sovent in the process. A ^{1}H NMR sample was prepared similarly from **2** (10 mg, 8.4×10^{-6} mol), CD_2Cl_2 (0.35 mL, originally 0.5 mL), $CDCl_2F$ (0.4 mL), and ethylene (15 mL). In the evacuated samples, the appearance of **19**, in place of **17**, was observed.

^{1}H NMR (400 MHz, CD_2Cl_2/$CDCl_2F$, −100 °C) δ 8.58 (d, J = 8 Hz, 1H, H$_c$ or H$_{c'}$), 8.51 (d, J = 4.7 Hz, 1H, H$_a$ or H$_{a'}$), 8.44 (d, J = 8.6 Hz, 1H, H$_{c'}$ or H$_c$), 8.31 (d, J = 4.7 Hz, 1H, H$_{a'}$ or H$_a$), 7.86 (s, 2H, H$_d$ and H$_{d'}$), 7.7 (m, 8H, Ar′-H$_o$), 7.5 (s, 4H, Ar′-H$_p$), 5.25 (br s, 4H, C$_2$H$_4$), 2.74 (s, 3H, CH$_3$). The resonances for H$_b$ and H$_{b'}$ overlap with H$_d$ and H$_{d'}$ and Ar′-H$_o$, as determined by integration.

^{13}C NMR (75 MHz, CD_2Cl_2, −95°) δ 223.0 (s, *C*(O)CH$_3$), 161.2 (q, $^1J_{CB}$ = 50 Hz, Ar′-C$_i$), 150.1 (d, J_{CH} = 186 Hz, C$_a$ or C$_{a'}$), 147.1 (d, J_{CH} = 181 Hz, C$_{a'}$ or C$_a$), 144.1 (s, C$_e$ or C$_{e'}$), 142.5 (s, C$_{e'}$ or C$_e$), 140.7 (d, J_{CH} = 170 Hz, C$_c$ or C$_{c'}$), 139.5 (d, J_{CH} = 166 Hz, C$_{c'}$ or C$_c$), 133.9 (d, J_{CH} = 159 Hz, Ar′-C$_o$), 129.6 (s, C$_f$ or C$_{f'}$), 129.4 (s, C$_{f'}$ or C$_f$), 127.9 (q, $^2J_{CF}$ = 29 Hz, Ar′-C$_m$), 127.4 (d, J_{CH} = 163 Hz, C$_d$ or C$_{d'}$), 127.0 (d, J_{CH} = 164 Hz, C$_{d'}$ or C$_d$), 125.4 (d, J_{CH} = 170 Hz, C$_b$ or C$_{b'}$), 125.3 (d, J_{CH} = 170 Hz, C$_{b'}$ or C$_b$), 123.6 (q, $^1J_{CF}$ = 273 Hz, Ar′-CF$_3$), 116.9 (d, J_{CH} = 166 Hz, Ar′-C$_p$), 94 (t, J_{CH} = 165(5) Hz, $w_{1/2}$ = 35 Hz, C$_2$H$_4$), 35.9 (q, J_{CH} = 131 Hz, CH$_3$).

(phen)Pd(CH$_2$CH$_2$C(O)CH$_3$)$^+$Ar′$_4$B$^-$ (14). Ethylene was purged through a solution of **2** (389 mg, 3.26×10^{-4} mol) and CH_2Cl_2 (10 mL) at 20 °C for 30 s. The color changed from light to intense yellow. The CH_2Cl_2 was removed *in vacuo* and the crude product dissolved in CH_2Cl_2 (1.5 mL) and cooled to −30 °C for ∼5 h; it was then cooled to −78 °C overnight, yielding yellow crystals. After the mother liquor was removed, the crystals were washed with hexanes (2 × 5 mL) and dried *in vacuo* giving **14** (252 mg, 63%) as a light yellow powder. Anal. Calcd for $C_{48}H_{27}BF_{24}N_2OPd$: C, 47.22; H, 2.23; N, 2.29. Found: C, 47.52; H, 1.92; N, 1.92.

IR (KBr) ν_{CO} = 1630 cm^{-1} (shoulder).

NMR spectral data are given in Tables 10 and 11.

Table 5. Equilibrium Constants for **14** + C_2H_4 ⇌ **15** from 181.1 to 216.5 K

temp (K)	K_3 (L·mol^{-1})	10^3[**14**]	10^3[**15**]	10^3[C_2H_4]
181.1	27.6	1.5	12.5	314
189.9	9.75	4.08	9.93	260
198.9	4.07	7.13	6.88	244
208.4	1.86	9.04	4.97	300
216.5	0.721	11.4	2.59	317

(phen)Pd(CH$_2$CH$_2$C(O)CH$_3$)(C$_2$H$_4$)$^+$Ar′$_4$B$^-$ (15). An aliquot (0.7 mL) of a CD_2Cl_2 solution of **14** (1.4×10^{-2} M) was added to a 5-mm NMR tube in the drybox. Ethylene (5 mL of gas) was added to the sample at −78 °C. The equilibrium constants and corresponding concentrations of reagents for the reaction **14** + C_2H_4 ⇌ **15**, determined from 181.1 to 216.5 K, are given in Table 5. The concentrations of the reagents were determined from the integrals of the −C**H**$_3$ resonances of **14** and **15** as follows:

$$[\mathbf{14}] = X(\mathbf{14}) \times 0.014\ \text{M} \qquad [\mathbf{15}] = X(\mathbf{15}) \times 0.014\ \text{M}$$

X(**14**) and X(**15**) are the mole fractions of **14** and **15**, respectively, determined from their integrals.

$$[C_2H_4] = [C_2H_4]_{total} - [\mathbf{15}]$$

(accounting for the the fast chemical exchange of free and coordinated ethylene resonances)

$$[C_2H_4]_{total} = \{[(C_2\mathbf{H}_4)/4]/[(\mathbf{14}\text{-}C\mathbf{H}_3 + \mathbf{15}\text{-}C\mathbf{H}_3)/3)\} \times 0.014\ \text{M}$$

The crude ethylene integral was corrected for that of the overlapped C**H**DCl$_2$ resonance before any other ethylene concentration calculations were performed.

Thermodynamic parameters were determined from a van't Hoff plot: $\Delta H° = -7.8 \pm 0.3$ kcal/mol, $\Delta S° = -36 \pm 1.5$ eu.

The ^{1}H NMR of **15** was recorded with this sample at 181.1 K (−92 °C). The ^{13}C NMR sample was prepared separately using **14** (20 mg, 1.6×10^{-5} mol), CD_2Cl_2 (0.7 mL), and C_2H_4 (10 mL of gas) at −78 °C, NMR (−90 °C); ^{1}H and ^{13}C NMR data are listed in Tables 10 and 11.

(phen)Pd(CH$_2$CH$_2$C(O)CH$_3$)(CO)$^+$Ar′$_4$B$^-$ (16). A ^{1}H NMR sample of **16** was prepared by purging a CD_2Cl_2 (0.7 mL) solution of **14** (10 mg, 8×10^{-6} mol) with CO at −78 °C for 5 min. The sample was placed in a precooled (−90 °C) NMR probe and a ^{1}H NMR spectrum was obtained. A ^{13}C NMR sample was prepared similarly from **14** (30 mg, 2.5×10^{-5} mol), but was purged with CO for 1 min. NMR data are listed in Tables 10 and 11.

(phen)Pd(C(O)CH$_2$CH$_2$C(O)CH$_3$)(C$_2$H$_4$)$^+$Ar′$_4$B$^-$ (17) and (phen)Pd(C(O)CH$_2$CH$_2$C(O)CH$_3$)$^+$Ar′$_4$B$^-$ (19). CD_2Cl_2 (0.7 mL) was added to a 5 mm NMR tube charged with **14** (10 mg, 8.4×10^{-6} mol) at −78 °C. After warming briefly to dissolve **14**, the sample was purged with CO at −78 °C for 5 min followed by Ar for 30 min, giving a mixture of (phen)Pd(CH$_2$CH$_2$C(O)CH$_3$)(CO)$^+$Ar′$_4$B$^-$, (**16**), **14**, **18** and (phen)Pd(C(O)CH$_2$CH$_2$C(O)CH$_3$)$^+$Ar′$_4$B$^-$ (**19**) at −66 °C. Upon warming to −25 °C, resonances for **14**, **16**, and **18** had dissappeared leaving **19** as the sole product. Ethylene (5 mL of gas, 23 equiv by integration) was added to **19** at −78 °C forming **17**. A ^{13}C NMR sample was prepared similarly from **14** (30 mg, 2.5×10^{-5} mol), CD_2Cl_2 (0.6 mL), and excess CO and ethylene as described. ^{1}H and ^{13}C NMR of **17** and **19** are presented in Tables 10 and 11.

(phen)Pd(C(O)CH$_2$CH$_2$C(O)CH$_3$)(CO)$^+$Ar′$_4$B$^-$ (18). A ^{1}H NMR sample of **18** was prepared by purging a CD_2Cl_2 (0.7 mL) solution of **14** (10 mg, 8.2×10^{-6} mol) with CO at −78 °C for 5 min and warming to 20 °C. A ^{13}C NMR sample was prepared similarly from **14** (30 mg, 2.5×10^{-5} mol). NMR data are listed in Tables 10 and 11.

19: Preparation of complex **19** is described with complex **17**.

20, 21: Preparation of complexes **20** and **21** is described in part II, Kinetics.

Saturated Ethylene Concentration in CD_2Cl_2 at 20 °C. A 0.030 M solution of cyclooctane in CD_2Cl_2 (2 mL) was prepared. Ethylene was purged through aliquots (0.7 mL) of these samples for 5 min. The ^{1}H NMR was recorded employing a 1-min delay between pulses and the ratio of ethylene to cycooctane was recorded. After correcting for

Table 6. Turnover Frequencies of Ethylene Dimerization by **7** from 248.5 to 302.1 K

temp (K)	k (s^{-1})	corr (r)	TOs followed	equiv of C_2H_4[a] initially present
302.1	4.4×10^{-2}	0.991	15.7	70
302.1	4.6×10^{-2}	0.999	22	44 (consumed)
285.1	6.7×10^{-3}	0.999	6.1	15
285.1	6.6×10^{-3}	0.997	14.1	43
271.6	1.0×10^{-3}	0.999	4.3	64
271.6	8.5×10^{-4}	0.991	7.3	32
259.2	2.6×10^{-4}	0.999	2.4	12
259.2	2.4×10^{-4}	0.999	1.5	36
248.5	5.3×10^{-5}	0.996	.9	19
248.5	4.1×10^{-5}	0.995	.4	8

[a] Equivalents of ethylene determined by integration relative to **7**.

the change in volume with the purge, the [ethylene] was determined; $[\text{ethylene}]_{sat} = 0.11 \pm 0.01$ M.

II. Kinetics Experiments. The β-Methyl Migratory Insertion Reaction of (phen)Pd(CH_3)(C_2H_4)$^+$ (3). CD_2Cl_2 (0.7 mL) was added to a 5-mm NMR tube charged with **1** (10 mg, 8.0×10^{-6} mol) at −78 °C. The solution was warmed briefly to dissolve **1**, then ethylene was added at −78 °C. The reaction proceeded to form **7** and propene. The decay of the CH_3 signal of **1** relative to the unchanging counterion Ar′-H_p at −24.7 °C was used to determine the first-order rate constant for the reaction. Spectra were recorded *ca*. every 5 min for the first hour and every 10 min for the second hour (∼3 half-lives). The rate constant was determined from the slope of the line created from $-\ln[\mathbf{3}\text{-}CH_3/\text{Ar'-}H_p]_t$ versus time. $k = (2.8 \pm 0.2) \times 10^{-4}$ s^{-1}, $\Delta G^{\ddagger}_{Me} = 18.5 \pm 0.1$ kcal/mol. This is the average rate constant when 20, 12, and 5 equiv of ethylene were in solution.

The β-Ethyl Migratory Insertion Reaction of (phen)Pd(CH_2CH_3)(C_2H_4)$^+$ (7). Five-millimeter NMR tubes were charged with **1** (10 mg, 8.0×10^{-6} mol). CD_2Cl_2 (0.7 mL) was added at −78 °C and the samples were warmed briefly to dissolve **1**. Samples were purged with ethylene at −78 °C for 15−30 s, then warmed to 5 °C in an ice bath prior to placement in the NMR probe. The sample for the 248.5 K run was the same used for the β-migratory insertion reaction of **3**. Turnover frequencies were determined from the slope of the least-squares line of butene formation, determined by the normalized integrals: $[(^1/_6 \times C\mathbf{H}_3CH{=}CHC\mathbf{H}_3 + {}^1/_3 \times C\mathbf{H}_3CH_2CH{=}CH)/{}^1/_2 \times PdC\mathbf{H}_2CH_3]$ versus time. The results are displayed in Table 6 and Figures 1 and 2. An Eyring plot created from $1000/T$ vs $\ln\{k/T\}$ gave $\Delta H^{\ddagger} = +18.5 \pm 0.6$ kcal/mol and $\Delta S^{\ddagger} = -3.7 \pm 2.0$ eu.

Butene composition was relatively constant when $[C_2H_4]$ was high: *trans*-2-butene, 60−65%; *cis*-2-butene, 30−35%; 1-butene, 5−10%. In one of the 302.1 K runs, complete ethylene consumption was allowed. The butene composition varied during the dimerization, favoring *trans*-2- at the expense of *cis*-2- and 1-butene as $[C_2H_4]$ decreased. After the ethylene was totally taken up in the 302.1 K run, complete butene conversion to higher order oligomers was observed.

The α-Methyl Migratory Insertion Reaction of (phen)Pd(CH_3)(CO)$^+$ (2). (a) Reaction with Methyl Acrylate Saturation Kinetics. As a representative example, a 5-mL solution of **2** in CD_2Cl_2 (1.14×10^{-2} M) was prepared in the drybox. Aliquots (0.70 mL, 8.0×10^{-6} mol) were syringed into 5-mm thin-walled NMR tubes and stored at −78 °C until used. Methyl acrylate (4, 6, 20, 40, 60 μL) was added to the cold samples. Samples were rapidly shaken and placed in a precooled (−66 °C) NMR probe. After the sample equilibrated at probe temperature for *ca.* 5 min, data acquisition was begun. The disappearance of the Pd-C$\mathbf{H}_3$ and the appearance of Pd−O=C(C$\mathbf{H}_3$)R signals were followed by ^{1}H NMR. No other species were observed. Spectra were obtained *ca.* every 5 min for the first hour and every 10 min afterwards for at least 2 half-lives. First-order rate constants were obtained as the slopes of the lines created from plots of $-\ln[(X(\mathbf{2})_t]$ versus time, where $X(\mathbf{2})$ is the mole fraction of **2** determined from the integrals of the CH_3 resonances of **2** and **9**. The results of this run and a separate run (solution was 1.17×10^{-2} M) were averaged together. Average concentrations of methyl acrylate and rate constants are shown in Table 7. The saturation rate constant is $k_{sat} = (2.4 \pm 0.3) \times 10^{-4}$ s^{-1}, $\Delta G^{\ddagger} = 15.4 \pm 0.1$ kcal/mol.

(b) Reaction of 2 with CO. A 5-mm thin-walled NMR tube was charged with **2** (10 mg, 8×10^{-6} mol) and CD_2Cl_2 (0.7 mL), then cooled to −78 °C and purged with CO for 4 min. The sample was placed in a precooled NMR probe (−66 °C). After 5 min, the conversion of **2** to **8** was monitored by the changing integrals of the methyl resonances in the ^{1}H NMR. The reaction went to 55% completion. The rate constant obtained during this period for the disappearance of **2** was obtained as the slope of the line created from the plot of time vs $-\ln[(X(\mathbf{2})_t]$. $X(\mathbf{2})$ is the mole fraction of **2** determined from the integrals of **2** and **8**. $k = 2.6 \times 10^{-4}$ s^{-1}, $\Delta G^{\ddagger} = 15.4 \pm 0.1$ kcal/mol. This experiment was repeated with a separate sample prepared from **3** (5.0 mg, 4.2×10^{-6} mol) and CD_2Cl_2 (0.7 mL), purged with CO for 4 min. The reaction was followed for 2 half-lives, $k = 2.2 \times 10^{-4}$ s^{-1}, $\Delta G^{\ddagger} = 15.4 \pm 0.1$ kcal/mol. $k_{av} = (2.4 \pm 0.2) \times 10^{-4}$ s^{-1}, $\Delta G^{\ddagger} = 15.4 \pm 0.1$ kcal/mol.

Carbonyl Scrambling: 2 + ^{13}CO → (phen)Pd(CH_3)(^{n}CO)$^+$ + (phen)Pd(^{n}C(O)CH_3)(^{n}CO)$^+$ (n = 12, 13). ^{13}CO was bubbled through a solution of (phen)Pd(CH_3)(CO)$^+$ (10 mg, 8×10^{-6} mol) and CD_2Cl_2 (0.7 mL) for 10 s at −78 °C in a 5 mm NMR tube. The sample was placed in a precooled (−66 °C) NMR probe and ^{1}H and ^{13}C{^{1}H} NMR spectra were recorded. The ^{13}C NMR spectra showed ^{13}CO resonances at δ 216.7 (**8** **C**(O)CH_3), 175.9 (**2** CO), and 173.0 (**8** CO). The ^{1}H NMR spectrum showed the presence of $^2J_{CH} = 5.9$ Hz satellites at δ 2.9 (^{13}C(O)CH_3).

Carbonyl Crossover Experiment: 2* + 12. A 5-mm NMR tube was charged with **2*** (10 mg, 8×10^{-6} mol) and **12** (10 mg, 8.6×10^{-6} mol). CD_2Cl_2 (0.7 mL) was added at −78 °C and the sample shaken briefly to dissolve the solids. The sample was placed in a precooled (−66 °C) NMR probe and the ^{13}C NMR monitored over a 4-h period. No crossover of the ^{13}C-labeled CO of **2*** (δ 175.9) into **4** (δ 175.7) was observed.

(c) Reaction of 2 with Ethylene Forms a Mixture of 3, 8, 13, 14, 15, and 17 (Scheme 3). (c.1) Pre- and Postequilibria between Ethylene and CO Binding. An aliquot (0.7 mL, 9.1×10^{-6} mol) of a CD_2Cl_2 solution of **2** (1.3×10^{-2} M) was added to a 5 mm NMR tube in the drybox. Ethylene (5 mL, ∼30 equiv) was added to the sample at −78 °C, which was then placed in a precooled (−66 °C) NMR probe; spectra were recorded after a 5-min delay. The ^{1}H NMR indicated that there were *ca.* 8 equiv of ethylene in solution. Two distinctive features of the subsequent spectra were the following: (1) The **2**-Me resonance was constantly broadened ($W-W_o \sim 13$ Hz) {broadening is dependent on $[C_2H_4]$} and its chemical shift remained constant. This indicated that the following preequilibrium was occurring (in the slow exchange regime):

$$\mathbf{2} + C_2H_4 \rightleftharpoons \mathbf{3} + CO$$

(2) The chemical shift of the acyl resonance steadily moved upfield from 2.804 to 2.747 as the reaction progressed (**8**-Me, δ 2.916; **13**-Me, δ 2.729) over the first 1.7 half-lives of the reaction. Thus, it is apparent that the CO formed in the preequilibrium displaces the C_2H_4 ligand in **13** to give a postequilibrium (in the fast exchange regime):

$$\mathbf{8} + C_2H_4 \rightleftharpoons \mathbf{13} + CO$$

These reactions are much faster (NMR time scale) than the migratory insertion. Therefore, these equilibria are driven to **13** as CO is consumed by the migratory insertion. Only after ∼1 half-life was [**3**] large enough to measure; even so, [CO] was too low to be accurately determined by conservation of mass. This prevented the direct measurement of the equilibrium constants and suggests that C_2H_4 is the dominant trapping ligand. However, an average ratio of the two was calculated from $K_2/K_1 = ([\mathbf{13}]/[\mathbf{8}])/([\mathbf{3}]/[\mathbf{2}])$ before **14**, **15**, or **17** were measurable. The mole fractions of **3**, **2**, **8**, and **13** were determined and their values used to compute the ratio. The ratio of **13**/**8** was determined at time = t from the position of the chemical shift:

$$[\mathbf{8}]_t = \{(\delta_t - \delta(\mathbf{13}\text{-Me}))[\mathbf{8} + \mathbf{13}]_t\}\{1/(\delta(\mathbf{8}\text{-Me}) - \delta(\mathbf{13}\text{-Me}))\}$$

$$[\mathbf{13}]_t = [\mathbf{8} + \mathbf{13}]_t - [\mathbf{8}]_t$$

Where δ_t is the time averaged chemical shift of **8** and **13** at time = t; $[\mathbf{8} + \mathbf{13}]_t$ is the total mole fraction of **8** and **13** at time = t. $K_2/K_1 = 34 \pm 4$.

Table 7. Summary of Kinetic Data for the Reaction of **2** with Methyl Acrylate (MA)

$10^4 k_{obs}$ (s^{-1})	[MA]	$10^4 k_{obs}$ (s^{-1})	[MA]
1.1	0.066 ± 0.01	2.45 ± 0.25	0.67 ± 0.04
1.4 ± 0.1	0.13 ± 0.03	2.4 ± 0.3	0.90 ± 0.04
1.95 ± 0.05	0.35 ± 0.02		

After 98% disappearance of **2** (*ca.* 4 h) the product distribution was **13** (78%), **14** (3%), **15** (1%), **17** (6%), and **3** (10%).

(c.2) Kinetics of the formation of (phen)Pd(C(O)CH$_3$)(C$_2$H$_4$)$^+$ (13) and (phen)Pd(C(O)CH$_3$)(CO)$^+$ (8). The concentration of **3**, **14**, **15**, or **17** was not measurable before 1 half-life of the reaction. This allowed the rate of product formation to be measured during the first half-life. The increase of the C(O)C**H**$_3$ signal of **8** + **13** relative to the unchanging counterion Ar′-H$_p$ at −66 °C was used to determine a first-order rate constant for the reaction. Spectra were recorded approximately every 5 min for 30 min. The rate constant for the appearance of **8** + **13** was determined from the slope of the line created from time versus $-\ln\{[(\mathbf{3}\text{-}CH_3)_{t=0}/Ar'\text{-}H_p] - [(\mathbf{8}+\mathbf{13}\text{-}CH_3)_t/Ar'\text{-}H_p]_t\}$ for the first 30 min (before [**3**] was measurable); note that $(\mathbf{3}\text{-}CH_3)_{t=0} = (\mathbf{8}+\mathbf{13}\text{-}CH_3)_\infty$. $k = (2.2 \pm 0.1) \times 10^{-4}$ s^{-1}, $\Delta G^\ddagger = 15.4 \pm 0.1$ kcal/mol. This rate constant is the average of two separate runs where 8 and 15 equiv of ethylene were in solution.

(c.3) The β-Acetyl Migratory Insertion of (phen)Pd(C(O)CH$_3$)(C$_2$H$_4$)$^+$ (13) in the Presence of Ethylene. The sample from Sections c.1 and c.2 was warmed to −46 °C and the conversion of **13** to **14** and **15** was observed. The disappearance of the **13**-C**H**$_3$ and appearance of the time-averaged **14** + **15**-C**H**$_3$ signals were followed by ^{1}H NMR. Spectra were obtained approximately every 5 min for the first hour and every 10 min afterwards for ∼3 half-lives. The rate constant for the decay of **13** was obtained as the slope of the line created from the plot of $-\ln[(X(\mathbf{13})_t]$ versus time. X(**13**) is the mole fraction of **13** determined from the integrals of **13** and **14** + **15**. $k = (4.8 \pm 0.5) \times 10^{-4}$ s^{-1}, $\Delta G^\ddagger = 16.6 \pm 0.1$ kcal/mol. This is the averaged rate constant for two separate runs where *ca.* 7 and 14 equiv of ethylene were present in solution, respectively.

(c.4) The β-Acetyl Migratory Insertion of (phen)Pd(C(O)CH$_3$)(C$_2$H$_4$)$^+$ (13) in the Absence of Ethylene. As a check of the invariance of the reaction rate to [ethylene], a sample of **13** was prepared and free ethylene removed as described previously for the ^{1}H NMR sample of **13**. The dissaopearance of **13** and the appearance of **14** were observed at −46 °C. Unlike in Section c.3, **19**, formed from **17** after ethylene loss, was observed (Scheme 6). The methyl resonance of **19** overlaps with that of **13**, preventing the accurate measurement of the integral of **13**. The rate constant for the appearance of **14** was obtained as the slope of the line created from the plot of $-\ln[(\mathbf{14}\text{-}CH_3/Ar'\text{-}H_p)_\infty - (\mathbf{14}\text{-}CH_3/Ar'\text{-}H_p)_t]$ versus time. k = 4.7×10^{-4} s^{-1}, $\Delta G^\ddagger = 16.6$ kcal/mol.

The β-Alkyl Migratory Insertion Reaction of (phen)Pd(CH$_2$CH$_2$C(O)CH$_3$)(CO)$^+$ (16) in the Presence of CO Forms (phen)Pd(C(O)CH$_2$CH$_2$C(O)CH$_3$)(CO)$^+$ (18) and (phen)Pd(C(O)CH$_2$CH$_2$C(O)CH$_3$)$^+$ (19). A ^{1}H NMR sample of **16** was prepared as described previously and placed in a precooled (−66 °C) NMR probe. After 5 min, the conversion of **16** to **18** + **19** was monitored by the changing integrals of the methyl resonances in the ^{1}H NMR spectra. The reaction was followed for 3.3 half-lives (Scheme 4, Figure 7). Complex **18** formed to 70% conversion, then halted sharply. Only then did complex **19** begin to form. The first order rate of decay of **16** equaled the rate of formation of the sum of **18** and **19**. The rate constant was determined as the slopes of the lines of $-\ln[X(\mathbf{16})]$ and $-\ln[1 - X(\mathbf{18}+\mathbf{19})]$ versus time; X(**16**), X(**18**), and X(**19**) are the mole fractions of **16**, **18**, and **19**, respectively. $k = 7.7 \times 10^{-4}$ s^{-1}, $\Delta G^\ddagger = 15.0 \pm 0.1$ kcal/mol.

The β-Alkyl Migratory Insertion Reaction of (phen)Pd(CH$_2$CH$_2$C(O)CH$_3$)-(CO)$^+$ (16) in the *Absence* of CO Forms (phen)Pd(C(O)CH$_2$CH$_2$C(O)CH$_3$)$^+$ (19). A ^{1}H NMR sample of **16** was was prepared by the addition of CO (5 min purge) to a sample of CD_2Cl_2 (0.7 mL) and **14** (10 mg, 8.2×10^{-6} mol) at −78 °C. Then the solution was purged with argon for 30 min to remove extra CO from the system. The sample was placed in a cold (−66 °C) NMR probe. The initial product distribution included **16** (23%), **19** (30%), **14** (24%), and **18** (23%). The concentrations of **14** and **18** changed only slightly (**14**, from 24 to 18%; **18**, from 23 to 21%) during the first 3 half-lives of the conversion of **16** to **19**. The rate constant was determined as the slopes of the lines of $-\ln[X(\mathbf{16})]$ and $-\ln[1 - X(\mathbf{19})]$ versus time; X(**16**) and X(**19**) are the mole fractions of **16** and **19**, respectively. $k = 8.5 \times 10^{-4}$ s^{-1}, $\Delta G^\ddagger = 14.9 \pm 0.1$ kcal/mol.

Reaction of (phen)Pd(C(O)CH$_2$CH$_2$^{13}C(O)CH$_3$)$^+$ (19*) with Ethylene. (a) Equilibrium with (phen)Pd(C(O)CH$_2$CH$_2$^{13}C(O)CH$_3$)(C$_2$H$_4$)$^+$ (17*). An aliquot (0.7 mL) of a CD_2Cl_2 solution of **14*** (9.0×10^{-3} M) (**14*** = ^{13}CO (99%) labeled **14**) was converted with CO and argon to **19*** as described previously for **19**. At −78 °C, ethylene (1 mL, *ca.* 3.5 equiv by integration) was added to the sample which was then placed in a cold (−83 °C) NMR (75 MHz ^{13}C) probe. The carbonyl resonances of **19*** (δ 222.1) and **17*** (δ 207.7) were in the fast exchange regime at 209.4 K and above. ^{1}H and ^{13}C{^{1}H} NMR were recorded at 209.4 and 218.4 K. Concentrations of **19*** and **17*** were determined from the population weighted averaged chemical shift: [**17***] = [**17*** + **19***]($\delta_{obs} - \delta_{21*}$)/($\delta_{19*} - \delta_{21*}$); [**19***] = [**17*** + **19***] − [**17***]. The ethylene concentration was determined using [ethylene] = {[**17*** + **19***](equiv of ethylene) − [**17***]} from integration (delay = 10 s) of the ^{1}H NMR spectrum. The K_{eq} was also evaluated at 228.8 K ([**17*** + **19***] = 1.5×10^{-2} M, 9 equiv of C_2H_4) immediately before the rate of conversion of **17*** to **20** and **21** was monitored, Section b, below. A van't Hoff plot of these data gave $\Delta H^\circ = -6.5 \pm 1.1$ kcal/mol and $\Delta S^\circ = -24 \pm 5$ eu.

Table 8. Equilibrium Constants for the Reaction **19*** + C_2H_4 ⇌ **17*** from 209.4 to 228.8 K

T (K)	δ_{obs}	10^3[ethylene]	10^3[**19***]	10^3[**17***]	K_4 (L·mol^{-1})
209.4	214.7	27	4.4	4.6	39.6
218.4	217.6	27	6.2	2.8	17.0
228.8	213.9	126	6.4	8.5	10.5

Table 9. Equilibrium Constants for the Reaction (phen)Pd(CH$_3$)(CO)$^+$ + S(CH$_3$)(C$_6$H$_5$) ⇌ (phen)Pd(CH$_3$)(S(CH$_3$)(C$_6$H$_5$))$^+$ + CO

[**2**]	[MeSPh]	[**4**]	[CO]$_{sat}$	K_A	ΔG°
0.023	.57	3.0×10^{-4}	0.0070	1.6×10^{-4}	3.3
0.025	.38	6.0×10^{-4}	0.0070	4.4×10^{-4}	2.9
0.010	.12	9.3×10^{-5}	0.0070	5.4×10^{-4}	2.85

(b) The β-Acyl Migratory Insertion Reaction of (phen)Pd(C(O)CH$_2$CH$_2$^{13}C(O)CH$_3$)(C$_2$H$_4$)$^+$ (17*). The sample used to obtain the K_{eq} at 228.8 K in Section a, above, ([**17*** + **19***] = 1.5×10^{-2} M, 9 equiv of C_2H_4 initially) was allowed to react at this temperature and form **20** and **21**. The rate of disappearance of the averaged methyl resonance of **17*** + **19*** (δ 2.4, $^2J_{CH}$ = 5.9 Hz) relative to the unchanging Ar′-H$_p$ resonance in the ^{1}H NMR spectra was monitored over time. The rate constant for the migratory insertion of **17*** was obtained from the slope of the plot of ln([**17*** + **19***]) versus time; the rate constant was calculated as $-\{\text{slope}/(K_{eq}[\text{ethylene}]/(1 + K_{eq}[\text{ethylene}])\}$, using [ethylene] = 0.1275 M (8.5 equiv): $k = 1.8 \times 10^{-4}$ s^{-1}, $\Delta G^\ddagger = 17.2 \pm 0.1$ kcal/mol.

^{1}H NMR of **20** + **21**: ^{1}H NMR (300 MHz, CD_2Cl_2, −44.4 °C) δ 8.9 (br m, 1H, H$_a$ or H$_{a'}$), 8.6 (br m, 3H, (H$_{a'}$ or H$_a$), H$_c$, H$_{c'}$), 7.95 (br m, 4H, H$_d$, H$_{d'}$, H$_b$, H$_{b'}$), 7.7 (m, 8H, Ar′-H$_o$), 7.55 (s, 4H, Ar′-H$_o$), 3.1 (br, 2H, CH$_2$), 2.9 (br, 4H, CH$_2$), 2.2 (br, 3H, CH$_3$).

The reaction of (phen)Pd(CH$_3$)(^{13}CO) (**2***) with C_2H_4 as described for **2** gave (phen)Pd(^{13}C(O)CH$_2$CH$_2$^{13}C(O)CH$_3$)(C$_2$H$_4$)$^+$ (**17****) which rearranged upon warming to ^{13}CO labeled **20** and **21**.

^{13}C NMR (75 MHz, CD_2Cl_2, −90 °C): δ 240.8 (Pd−O=CR−, **21**), 211.3 (RC(O)R, **20**), 207.8 (RC(O)R, **20**), 206.9 (RC(O)R, **21**).

III. Equilibrium Experiments. In the following NMR experiments, a relaxation delay of 10 s between pulses was employed.

Measurement of Relative Equilbrium Constants. (a) K_2/K_1. Calculation of the ratio K_2/K_1 is described previously during the reaction of **2** with ethylene.

(b) K_5/K_1. A 5-mm NMR tube was charged with a 0.015 M CD_2Cl_2 (0.7 mL) solution of ^{13}CO-labeled **14**. The solution was cooled to −78 °C and purged with ^{12}CO for *ca.* 5 min and then argon for 30 min. The sample was placed in a −25 °C NMR probe where **19*** was formed. The sample was returned to the −78 °C bath and *ca.* half of the solution was replaced with a separate solution of CD_2Cl_2 (0.8 mL) and **2** (11 mg, 9×10^{-6} mol). Next, ethylene (2.5 mL of gas, 8.4 equiv, by integration) was added at −78 °C. The sample was then placed in a −83 °C NMR probe. A ^{13}C NMR spectrum revealed one broad ($W_{1/2}$ = 65 Hz) ^{13}C enriched carbonyl resonance at δ 208.1. The methyl signals of the ^{1}H NMR spectrum contained a mixture of **17*** + **18*** (averaged resonance, 50.9%), **3** (13.6%), and **2** (35.6%). The ratio K_5/K_1 (=7.2) was determined as described in the text.

Table 10. ^{1}H NMR Data for Complexes **14**−**19** in CD_2Cl_2

X	$H_{a,a'}$	$H_{b,b'}$	$H_{c,c'}$	$H_{d,d'}$	CH_2	$C(O)CH_3$
14 (20 °C)	9.12 (dd, 4.83, 1.39 Hz) 8.6 (m)	7.99 (dd, 8.29, 4.83 Hz) 7.85 (dd, 8.14, 5.37 Hz)	8.64 (m)	8.09 (d, 8.9 Hz) 8.03 (d, 8.9 Hz)	3.71 (t, 6.38 Hz) 2.68 (t, 6.38 Hz)	2.50
15[a] (−92 °C)	8.84 (d, 4.74 Hz) 8.40 (d, 4.54 Hz)	7.95 (under Hd,d′) 7.86 (dd, 8.17, 4.87 Hz)	8.60 (d, 8.13 Hz) 8.51 (d, 8.00 Hz)	7.95	2.77 (t, 7.12 Hz) 1.74 (t, 7.12 Hz)	2.14
16 (−90 °C)	8.9 (m)	7.98 (dd, 8.2, 5.0 Hz) 7.83 (dd, 8.2, 5.0 Hz)	8.56 (d, 8.2 Hz) 8.50 (d, 8.2 Hz)	7.92 (d, 9.1 Hz) 7.90 (d, 9.1 Hz)	2.81 (br t, 6 Hz) 2.39 (br t, 6 Hz)	2.08
17[a] (−90 °C)	9.05 (d, 5 Hz) 8.34 (br d, 4 Hz)	8.00 (dd, 8, 5 Hz) 7.82 (dd, 8, 5 Hz)	8.59 (d, 8 Hz) 8.45 (d, 8 Hz)	7.94 (d, 8.9 Hz) 7.91 (d, 8.9 Hz)	3.17 (m) 2.74 (m)	2.18
18 (−75 °C)	8.91 (d, 5.1 Hz) 8.77 (d, 4.9 Hz)	8.00 (dd, 8.4, 5.1 Hz) 7.86 (dd, 8.2, 4.9 Hz)	8.63 (d, 8.2 Hz) 8.54 (d, 8.4 Hz)	7.97 (s)	3.32 (m) 2.88 (m)	2.20
19 (−66 °C)	9.06 (d, 5.0 Hz) 8.26 (d, 5.0 Hz)	7.95 (dd, 8.4, 5.0 Hz) 7.40 (dd, 8.4, 5.0 Hz)	8.49 (d, 8.4 Hz) 8.16 (d, 8.4 Hz)	7.75 (under Ar′-H_o)	2.98 (br t, 6 Hz) 2.58 (br t, 6 Hz)	2.74

[a] The ethylene resonances of **15** and **17** are averaged with free ethylene: **15** (*ca.* 25 equiv of ethylene); **17** (*ca.* 20 equiv of ethylene).

Table 11. ^{13}C NMR Data for Complexes **14**−**19** in CD_2Cl_2

X	CO	$C_{a,a'}$	$C_{e,e'}$	$C_{c,c'}$	$C_{f,f'}$	$C_{b,b'}$	$C_{d,d'}$	CH_2	$C(O)\mathbf{C}H_3$
14 (20 °C)	240.9	151.5 (d, 185 Hz) 149.6 (d, 184 Hz)	148.0 144.3	139.9 (d, 168 Hz) 139.3 (d, 167 Hz)	131.1 130.5	128.2 (d, 167 Hz) 127.7 (d, 167 Hz)	126.5 (d, 169 Hz) 126.4 (d, 171 Hz)	51.1 (t, 126 Hz) 23.1 (t, 138 Hz)	28.0 (q, 130 Hz)
15[a] (−92 °C)	213.1	146.9 (d, 182 Hz) 146.6 (d, 180 Hz)	145.5 143.6	140.1 (d, 167 Hz) 139.3 (d, 168 Hz)	130.0 129.8	127.4 (d, 167 Hz) 127.3 (d, 167 Hz)	125.5 (d, 170 Hz) 125.3 (d, 171 Hz)	45.3 (t, 126 Hz) 25.9 (t, 140 Hz)	29.6 (q, 129 Hz)
16 (−90 °C)	207.7 176.5	150.9 (d, 185 Hz) 147.2 (d, 183 Hz)	146.6 143.0	140.1 (d, 167 Hz) 139.3 (d, 168 Hz)	130.2 129.8	127.7 (d, 167 Hz) 127.2 (d, 163 Hz)	126.1 (d, 171 Hz) 125.5 (d, 171 Hz)	43.5 (t, 125 Hz) 17.1 (t, 140 Hz)	29.6 (q, 127 Hz)
17[a] (−90 °C)	220.5 207.7	151.6 (d, 184 Hz) 147.2 (d, 179 Hz)	144.3 142.8	140.4 (d, 167 Hz) 139.6 (d, 168 Hz)	129.7 129.6	127.3 (d, 167 Hz)	125.6 (d, 170 Hz) 125.3 (d, 170 Hz)	43.2 (t, 131 Hz) 38.3 (t, 129 Hz)	29.5 (q, 128 Hz)
18 (−83 °C)	217.9 207.2 172.7	152.2 (d, 188 Hz) 150.8 (d, 184 Hz)	144.9 142.7	140.9 (d, 168 Hz) 140.0 (d, 168 Hz)	129.71 129.68	127.4 (d, 168 Hz) 127.3 (d, 168 Hz)	125.8 (d, 171 Hz) 125.7 (d, 171 Hz)	48.8 (t, 133 Hz) 38.9 (t, 128 Hz)	29.2 (q, 127 Hz)
19 (−90 °C)	222.1 220.7	149.2 (d, 189 Hz) 146.1 (d, 186 Hz)	144.3 141.2	139.8 (d, 167 Hz) 138.2 (d, 167 Hz)	129.4 129.3	126.7 (d, 170 Hz)	124.7 (d, 169 Hz) 124.2 (d, 168 Hz)	35.8 (t, 130 Hz) 30.8 (t, 135 Hz)	31.9 (q, 130 Hz)

(c) K_6/K_1. A 5 mm NMR tube was charged with **2** (11 mg, 9 × 10^{-6} mol) and **14** (11 mg, 9 × 10^{-6} mol). CD_2Cl_2 was added at −78 °C and the sample warmed briefly to dissolve the solids. Ethylene (2.5 mL of gas, 5.8 equiv by integration) was added and the sample placed in a precooled (−83 °C) NMR probe. The ^{1}H NMR spectrum contained a mixture of **2** (23.7%), **3** (29.3%), **14** (5.1%), **15** (8.7%), **16** (21.5%), **17** + **18** (6.0%) and **19** (5.8%). The ratio K_6/K_1 (=0.33) was determined as described in the text.

Relative Binding Affinity Studys. (K_A) (phen)Pd(CH_3)(CO)$^+$ + S(CH_3)(C_6H_5) ⇌ (phen)Pd(CH_3)(S(CH_3)(C_6H_5))$^+$ + CO. CD_2Cl_2 (0.7 mL) was added to a 5-mm NMR tube charged with **2** (25 mg, 2.0 × 10^{-5} mol; 10 mg, 8.0 × 10^{-6} mol) at −78 °C. The sample was warmed briefly to dissolve **2**. Thioanisole was added at −78 °C; the sample was shaken in rapid bursts and returned to the −78 °C bath to dissolve the frozen thioanisole. The 25-mg sample was purged with CO for 1 min and the 10-mg sample for 5 min at −78 °C (longer periods of time caused the 25-mg sample to precipitate analyte), and then the sample was placed in a −83 °C probe (relaxation delay = 10 s) where the equilibrium constants were determined using $[CO]_{sat}(-83°C) = 7.0 \times 10^{-3}$ M, calculated from Bryndza's formula. The concentrations of **2** and **4** were corrected for the small amount of (phen)Pd(C(O)CH_3)(S(CH_3)(C_6H_5))$^+$, acetyl methyl δ 2.19, formed from the initial addition of thioanisole. This gave $K_A = (3.8 \pm 1.6) \times 10^{-4}$, $\Delta G° = 3.0 \pm 0.2$ kcal/mol at −83 °C.

(K_B) (phen)Pd(CH_3)(S(CH_3)(C_6H_5))$^+$ + $NCCH_3$ ⇌ (phen)Pd(CH_3)($NCCH_3$)$^+$ + S(CH_3)(C_6H_5). An 11.66 mol % solution of $NCCH_3$ (270.3 mg, 6.585 × 10^{-3} mol) and $NCCD_3$ (2.1974 g, 4.986 × 10^{-2} mol) was prepared in a 3-mL volumetric flask. An aliquot (15 μL, 25 μL) of this mixture was added to a solution of **4** (10 mg, 8 × 10^{-6} mol) and the equilibrium constants (15 μL, 36.66 equiv, K = 6.54 × 10^{-3}, $\Delta G°$ = 2.07 kcal/mol; 25 μL, 62.2 equiv, K = 7.07 × 10^{-3}, $\Delta G°$ = 2.04 kcal/mol) determined at −66 °C.

(K_D) (phen)Pd(CH_3)(NCC_6H_5)$^+$ + C_2H_4 ⇌ (phen)Pd(CH_3)(C_2H_4)$^+$ + NCC_6H_5. Ethylene (0.2 mL, 0.4 mL) was added to a solution of CD_2Cl_2 (0.7 mL) and **6** (10 mg, 8 × 10^{-6} mol) at −78 °C and the equilibrium constants (0.2 mL, 0.55 equiv, K = 1.43, $\Delta G°$ = −0.15 kcal/mol; 0.4 mL, 1.4 equiv, K = 1.69, $\Delta G°$ = −0.22 kcal/mol) determined at −66 °C.

(K_E) (phen)Pd(CH_3)($NCCH_3$)$^+$ + NCC_6H_5 ⇌ (phen)Pd(CH_3)(NCC_6H_5)$^+$ + $NCCH_3$. Benzonitrile (1 μL, 1.5 μL) was added to a solution of CD_2Cl_2 (0.7 mL) and **5** (7 mg, 6 × 10^{-6} mol) and the equilibrium constants (1 μL, 1.5 equiv, K = 0.62, $\Delta G°$ = 0.20 kcal/mol; 1.5 μL, 2.5 equiv, K = 0.48, $\Delta G°$ = 0.30 kcal/mol) determined at −66 °C.

IV. X-ray Structure Determination of 8·CH_2Cl_2. Data were collected on a Rigaku AFC 6/S diffractometer with graphite-monochromated Mo Kα radiation (λ = 0.71073 Å) using a $\theta/2\theta$ scan; reflections with $I > 2.5\sigma$ were considered observed and included in subsequent calculations. The structures were solved by direct methods. Refinement was by full-matrix least squares with weights based on counter statistics. Hydrogen atoms were included in the final refinement using a riding model with thermal parameters derived from the atom to which they are bonded. Crystal data and experimental conditions are given in the supporting information. All computations were performed using the NRCVAX suite of programs.[70,71]

Acknowledgment. We are grateful to the Department of Energy (FG05-94ER14459) and the National Science Foundation (CHE-9412095) for financial[70] support of this work. F.C.R. was supported in part by a Department of Education Fellowship.

Supporting Information Available: Tables listing crystal data, collection parameters, and complete atomic coordinates, Bisos, bond distances, and angles for **8**·CH_2Cl_2 (6 pages). This material is contained in libraries on microfiche, immediately follows this article in the microfilm version of the journal, can be ordered from the ACS, and can be downloaded from the Internet; see any current masthead page for ordering information and Internet access instructions.

JA953276T

(70) Gabe, E. J.; Le Page, Y.; Charland, J.-P.; Lee, F.; White, P. S. *J. Appl. Crystallogr.* **1989**, *22*, 384.
(71) Johnson, C. K. Technical Report No. ORNL-5138, 1976; Oak Ridge National Laboratory: Oak Ridge, TN.